NRC Research Press

ARTICLE

Taxonomy and distribution of bottlenose dolphins (genus *Tursiops*) in Australian waters: an osteological clarification

M. Jedensjö, C.M. Kemper, M. Milella, E.P. Willems, and M. Krützen

Can. J. Zool. Downloaded from www.nrcresearchpress.com by Dr Maria Jedensjo on 06/24/20
For personal use only.

Abstract: Species relationships in the bottlenose dolphin (genus *Tursiops* Gervais, 1855) are controversial. We carried out a comprehensive osteological study of 264 skulls, including type specimens, and 90 postcranial skeletons of *Tursiops* spp. to address taxonomic uncertainties in Australia using two-dimensional (2D) measurements, and three-dimensional geometric morphometrics (3DGM), tooth and vertebral counts, and categorical data. Analyses provided support for the presence of two forms, aligned to the Indo-Pacific bottlenose dolphin (*Tursiops aduncus* (Ehrenberg, 1832)) and the common bottlenose dolphin (*Tursiops truncatus* (Montagu, 1821)), including type specimens. The Burrunan dolphin (*Tursiops australis* Charlton-Robb, Gershwin, Thompson, Austin, Owen and McKechnie, 2011) fell well within *T. truncatus* for both 2D and 3DGM methods. Thirteen *Tursiops* spp. specimens, no *T. australis* specimens, were of intermediate size (2D) and could not be assigned to either species. For 3DGM data, there was a strong allometric influence and few non-allometric differences between species. Length and width of the cranium and rostrum were important discriminating variables. *Tursiops aduncus* was smaller, had more teeth, fewer vertebrae, and more erosion on the pterygoids and frontals than *T. truncatus*. Overall cranium shape was round in *T. aduncus* and angular in *T. truncatus*. Skull length of *T. aduncus* was smaller in low than in high latitudes. This study highlights the importance of large sample size, multiple analytical methods, and extensive geographical coverage when undertaking taxonomic studies.

Key words: Tursiops truncatus, common bottlenose dolphin, *Tursiops aduncus*, Indo-Pacific bottlenose dolphin, *Tursiops australis*, Burrunan dolphin, bottlenose dolphin, morphology, geometric morphometrics, type specimens.

Résumé : Les relations entre espèces du grand dauphin (genre *Tursiops* Gervais, 1855) suscitent la controverse. Nous avons réalisé une étude ostéologique exhaustive de 264 crânes, dont des spécimens types, et de 90 squelettes postcrâniens de *Tursiops* spp., afin d'examiner des incertitudes taxonomiques relevées en Australie, en utilisant des mesures en deux dimensions (2D), ainsi que la morphométrie géométrique tridimensionnelle (MG3D), des comptes de dents et de vertèbres et des données catégorielles. Les analyses appuient la présence de deux formes, alignées avec le grand dauphin de l'indo-pacifique (*Tursiops aduncus* (Ehrenberg, 1833)) et le grand dauphin commun (*Tursiops truncatus* (Montagu, 1821)), incluant des spécimens types. Les deux méthodes (2D et MG3D) placent le dauphin Burrunan (*Tursiops australis* Charlton-Robb, Gershwin, Thompson, Austin, Owen et McKechnie, 2011) résolument au sein de *T. truncatus*. Treize spécimens de *Tursiops* spp., mais aucun spécimen de *T. australis*, sont de taille intermédiaire (2D) et ne peuvent être affectés à l'une ou l'autre des espèces. En ce qui concerne les données de MG3D, elles révèlent une forte influence allométrique et peu de différences non allométriques entre les espèces. La longueur et la largeur du crâne et du rostre sont d'importantes variables discriminantes. *Tursiops aduncus* est plus petit, compte plus de dents et moins de vertèbres et présente plus d'érosion sur les os ptérygoïdes et frontaux que *T. truncatus*. La forme générale du crâne de *T. aduncus* est ronde et celle de *T. truncatus*, angulaire. La longueur du crâne de *T. aduncus* est moins grande à basses latitudes qu'à hautes latitudes. L'étude souligne l'importance d'échantillons de grande taille et de l'utilisation de plusieurs méthodes analytiques et d'une grande couverture géographique pour les études taxonomiques. [Traduit par la Rédaction]

Mots-clés : Tursiops truncatus, grand dauphin commun, *Tursiops aduncus*, grand dauphin de l'indo-pacifique, *Tursiops australis*, dauphin Burrunan, grand dauphin, morphologie, morphométrie géométrique, spécimens types.

Introduction

The bottlenose dolphin (genus *Tursiops* Gervais, 1855) belongs to the most speciose family of Cetacea, the Delphinidae (Rice 1998). Relationships within this family have been widely debated (McGowen 2011; Perrin et al. 2013). For example, genetic studies concluded that the Indo-Pacific bottlenose dolphin (*Tursiops aduncus* (Ehrenberg, 1832)) and the common bottlenose dolphin (*Tursiops truncatus* (Montagu, 1821)) may be more closely related to other genera than to each other (LeDuc et al. 1999; Kingston et al. 2009; Moura et al. 2013). The challenge for understanding relationships within delphinids may be due to their rapid radiation (McGowen 2011; Perrin et al. 2013), difficulties in resolving short branches produced by cladistic analyses (McGowen 2011), incomplete lineage sorting (Nikaido et al. 2007; Perrin et al. 2013), and the difficulty identifying clear diagnostic morphological characters (Buchholtz and

Received 13 October 2018. Accepted 6 March 2020.

M. Jedensjö. Department of Anthropology, University of Zurich, Museum of Anthropology, Winterthurerstrasse 190, 8057 Zurich, Switzerland; South Australian Museum, North Terrace, Adelaide, SA 5000, Australia.
C.M. Kemper. South Australian Museum, North Terrace, Adelaide, SA 5000, Australia.
M. Milella. Department of Anthropology, University of Zurich, Museum of Anthropology, Winterthurerstrasse 190, 8057 Zurich, Switzerland; Department of Anthropology, Institute of Forensic Medicine, University of Bern, Bühlstrasse 20, 3012 Bern, Switzerland.
E.P. Willems and M. Krützen. Department of Anthropology, University of Zurich, Museum of Anthropology, Winterthurerstrasse 190, 8057 Zurich, Switzerland.

Corresponding author: Maria Jedensjö (email: m_jedensjo@hotmail.com).

Copyright remains with the author(s) or their institution(s). Permission for reuse (free in most cases) can be obtained from copyright.com.

Table 1. Number of bottlenose dolphin (*Tursiops* spp.) specimens examined in the study.

Specimen	F	M	UK	Total 2D	Total 3DGM	Vertebral count	Categorical data	Tooth count
Tursiops spp.	64	57	116	237	197	83	148	148
Tursiops australis	5	3	13	21	11	6		19
Delphinus truncatus (holotype, *Tursiops truncatus*, NHMUK 353a)	0	0	1	1	1	0	1	1
Delphinus aduncus (holotype, *Tursiops aduncus*, BZM 66400)	0	0	1	1	1	0	1	1
Tursiops australis (paralectotype, *T. truncatus* QVM 1365)	1	0	0	1	1	0	1	1
Tursiops maugeanus (junior synonym of *T. truncatus*, *T. truncatus*, QVM 1360)	0	1	0	1	1	1	1	1
Delphinus catalania (syntype, *T. aduncus*, NHMUK 1862.6.6.13, 14)	2	0	0	2	1	0	2	1
Total	72	61	131	264	213	90	154	172

Note: Two-dimensional (2D) linear measurements and three-dimensional geometric morphometric (3DGM) data were obtained. Due to missing data, not all specimens were used in each analysis. F, number of females; M, number of males; UK, unknown sex.

Can. J. Zool. Downloaded from www.nrcresearchpress.com by Dr Maria Jedensjo on 06/24/20
For personal use only.

Schur 2004; Amaral et al. 2009; Perrin et al. 2013). However, linear and geometric morphometric analysis show evidence of clear separation between *Tursiops* and some other delphinid genera (Amaral et al. 2009; Jedensjö et al. 2017).

In the past, at least 20 *Tursiops* spp. have been named (Rice 1998), but only two are currently recognised worldwide (Committee on Taxonomy 2018): *T. truncatus* and *T. aduncus*. Although Kinze (2018) concluded that *Tursiops tursio* (Gunnerus, 1768) predates *T. truncatus*, the present study will use the more universally adopted latter name. Another species, the Burrunan dolphin (*Tursiops australis* Charlton-Robb, Gershwin, Thompson, Austin, Owen and McKechnie, 2011), found in parts of southern Australia (Charlton-Robb et al. 2011), has not been widely accepted as a distinctive nominal species of *Tursiops* (Committee on Taxonomy 2018). Some authors (Möller et al. 2008; Moura et al. 2013) use the common name southern Australian bottlenose dolphin (SABD; for abbreviations see Appendix A, Table A1), which they have assumed to be *T. australis*.

Previous morphological studies have confirmed the occurrence of two *Tursiops* spp. in South Africa (Ross 1977, 1984), the Indian and western Pacific Ocean (Kurihara and Oda 2007), China (Wang et al. 2000*a*, 2000*b*; Natoli et al. 2004), Japan (Kakuda et al. 2002), and Australia (Hale et al. 2000; Kemper 2004). Distinction between these is sometimes based on size (Ross 1977; Wang et al. 2000*a*), where body length of *T. truncatus* is usually greater than 2.4 m (Wells and Scott 1999; Reeves et al. 2002), and *T. aduncus* is less than 2.6 m (Reeves et al. 2002). Skull characteristics have also proven informative, but without complete concordance between geographic regions (Ross 1977; Wang et al. 2000*a*), where skull size is generally larger in *T. truncatus* (Ross 1977; Wang et al. 2000*b*; Kemper 2004). However, an overlap in skull size has been reported for the China Sea (Wang et al. 2000*a*, 2000*b*) and South Australia (Kemper 2004).

Ross and Cockcroft (1990) examined external morphology and skeletons of *Tursiops* from Australia and provided evidence for a single species, *T. truncatus*, with clinal variation from north to south. Small specimens were found in the warm waters of northern Australia and larger ones in the cold south. Hale et al. (2000) described two distinct forms of *Tursiops* in southeastern Queensland: a large unspotted form in waters greater than 30 m deep (*T. truncatus*) and a small spotted form in waters less than 30 m deep (*Tursiops* cf. *aduncus*). Using multivariate analyses of skull measurements and features, Kemper (2004) found support for two morphotypes of bottlenose dolphins in South Australia. These had affinities with *T. aduncus* and *T. truncatus*. There is a need for a large-scale investigation to confirm the presence of these two species from other locations.

Bottlenose dolphin type specimens collected from Australia include two skulls of *Delphinus catalania* Gray, 1862, collected by John MacGillivray in 1860 at Cape Melville, Queensland, and two skulls of *Tursiops maugeanus* Iredale and Troughton, 1934, collected at Tamar River, Tasmania, in 1960 and 1965. Hershkovitz (1966) synonymised these species with *Tursiops truncatus aduncus*.

The aim of the present study was to investigate the taxonomy and distribution of bottlenose dolphins in Australia using a large data set from a broad geographic area. Classical, linear two-dimensional (2D) data were collected from skulls and counts were made of vertebrae. These data allowed comparison with previous studies. Three-dimensional geometric morphometric (3DGM) data were collected from skulls to provide a more detailed analysis of the relative contribution of allometric and non-allometric factors. Type specimens relevant to the Australian region were included in the study.

Materials and methods

Specimens

Data were obtained from Australian specimens ($n = 264$) held at nine Australian museums, the Natural History Museum (London, UK), and the Museum für Naturkunde (Berlin, Germany) (Table 1 and Supplementary material S1[1]). Specimens were collected between 1862 and 2009. Only those that were cranially mature were examined, in which the posterior maxillae were securely fused (i.e., no movement) to the cranium (Ross and Cockcroft 1990) and the suture closed or closing (Kemper 2004). Twenty-two specimens were previously identified as *T. australis* (Supplementary material S1)[1] by Charlton-Robb et al. (2011). Holotypes of *T. truncatus* (*Delphinus truncatus* Montagu, 1821) and *T. aduncus* (*Delphinus aduncus* Ehrenberg, 1832) were examined, as well as type specimens of other *Tursiops* taxa described from Australia (i.e., *Delphinus catalania* and *Tursiops maugeanus*; Table 1 and Supplementary material S1[1]). It is worth noting that one of the *T. maugeanus* syntypes became a junior synonym of *T. truncatus*, while the other became a paralectotype, *T. australis* (Charlton-Robb et al. 2011).

Two-dimensional, count, and categorical data collection and statistical protocols

Two-dimensional data (Table 1 and Supplementary materials S1 and S2[1]) were collected by M.J. and C.M.K., including 52 skull measurements (Fig. 1 and Appendix A, Table A1), 11 count (Appendix A, Table A1), and 10 categorical variables (Appendix A, Table A2). Most specimens from Western Australian Museum and South Australian Museum were measured by C.M.K. (excluding counts and categorical variables), while M.J. measured the specimens from other museums and type specimens. To calibrate measuring methods, M.J. was trained by C.M.K. and a Student's paired *t* test was used to test the differences between these. All skulls were measured twice by each person. Ten variables (GLPT, GWIN, GWPX, LAL, LO, MINDTF, RW60, RW75%, RWB, and RWM) showed a significant difference and were therefore re-measured by M.J. for all specimens from Western Australian Museum and South

[1]Supplementary materials S1–S4 are available with the article through the journal Web site at http://nrcresearchpress.com/doi/suppl/10.1139/cjz-2018-0270.

Fig. 1. Bottlenose dolphin (*Tursiops* spp.) skull measurements used in this study. Measurements ATW, GWAO, ILB, MINDTF, TLL, TLR, TRPS, TUL, TUR, and WAS are not illustrated. For abbreviation definitions see Appendix A, Table A2. The illustrated skull is *Tursiops* SAMA M20744 (modified from Kemper 2004, reproduced with permission of Aust. J. Zool., Vol. 52, p. 32, ©2004 CSIRO Publishing).

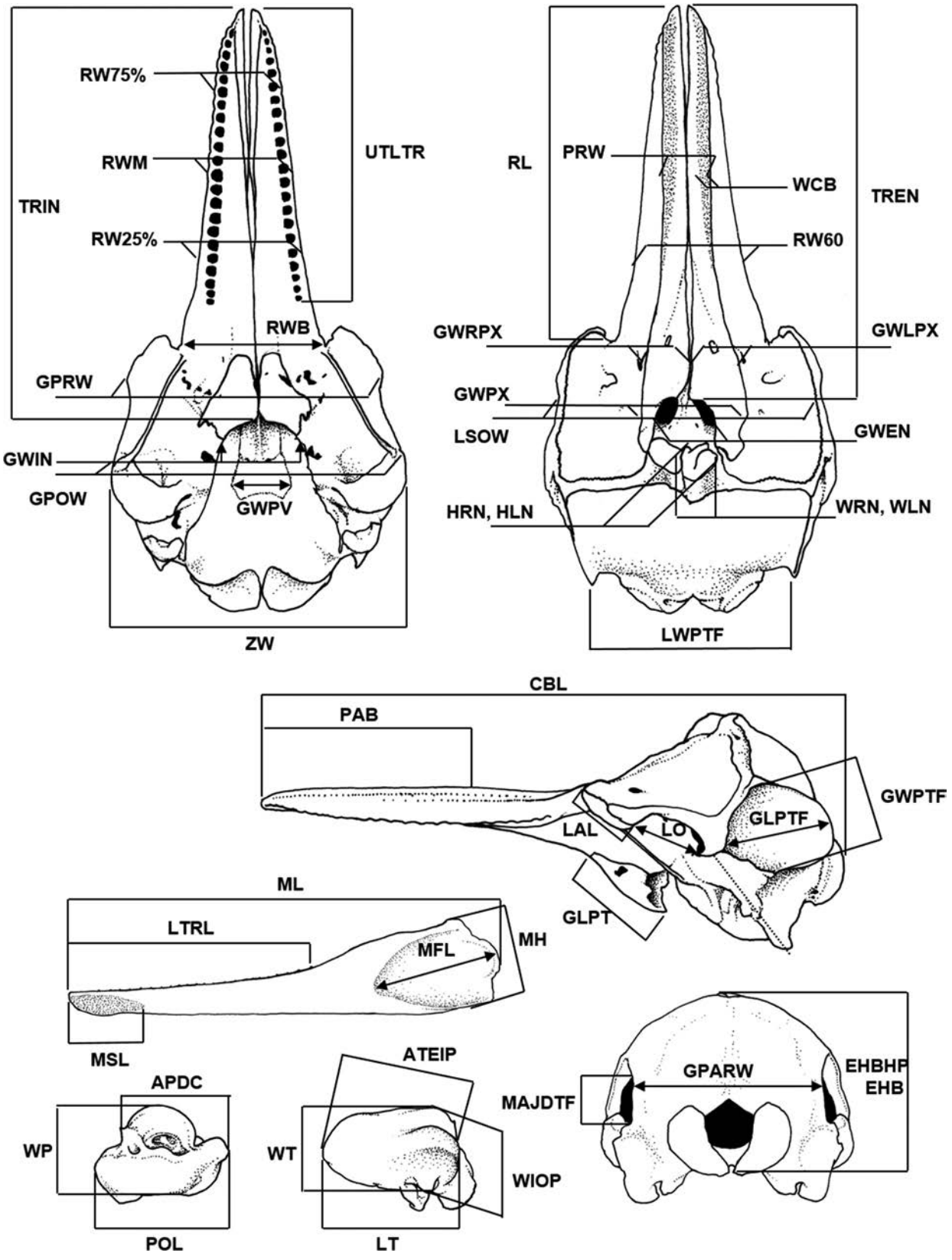

Can. J. Zool. Downloaded from www.nrcresearchpress.com by Dr Maria Jedensjo on 06/24/20
For personal use only.

Fig. 2. Landmark configuration (n = 73) for (A) dorsal, (B) ventral, (C) posterior, and (D) lateral views of a bottlenose dolphin (*Tursiops* spp.) skull (see Appendix A, Table A4). Landmarks 35, 49–53, and 59 were located on right side but here are viewed on left side. Illustrated skull is *Tursiops* SAMA M20744 (modified from Kemper 2004, reproduced with permission of Aust. J. Zool., Vol. 52, p. 32, ©2004 CSIRO Publishing.

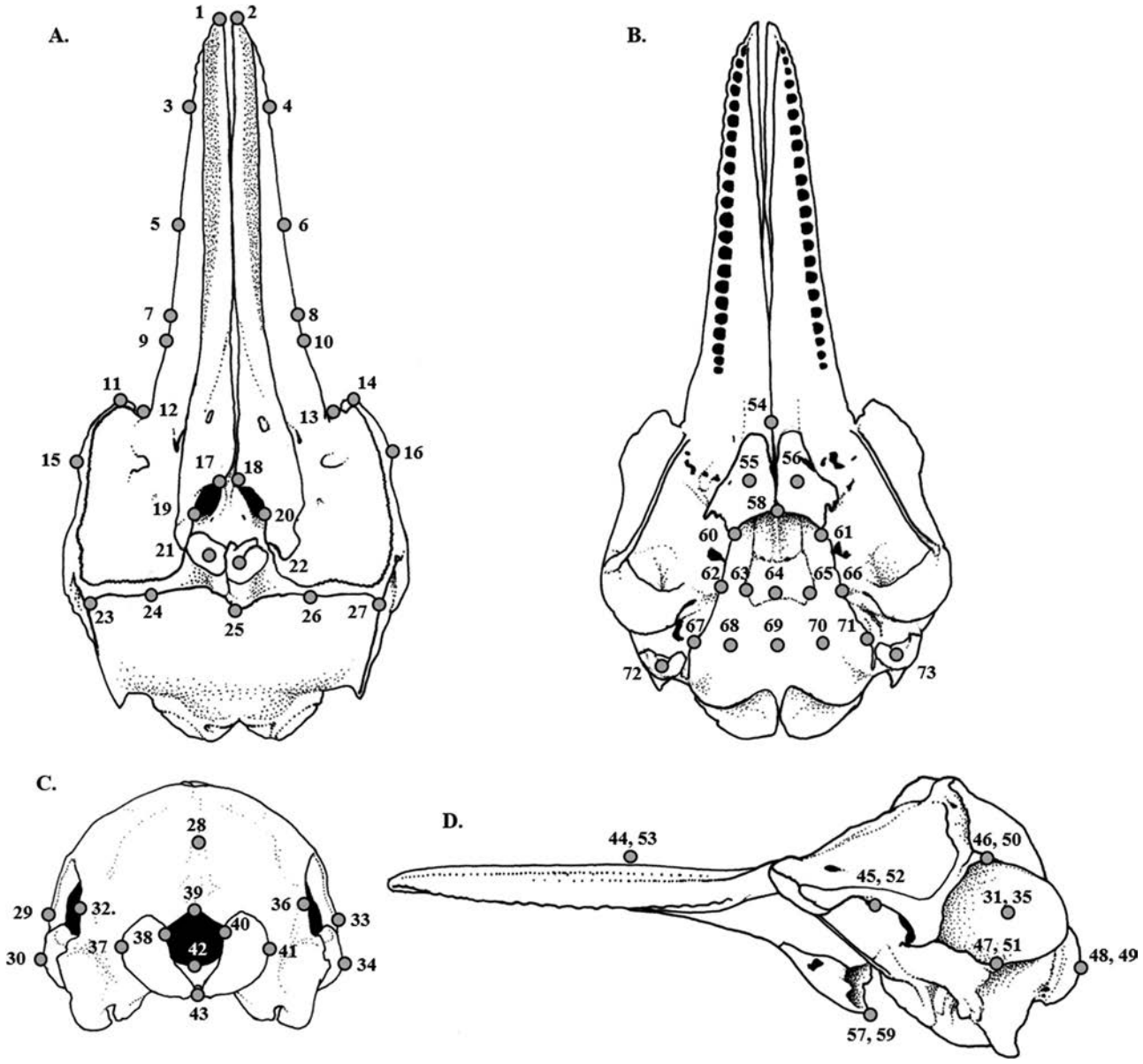

Australian Museum. Skull measurements were taken with anthropometers and spreading calipers to the nearest millimetre. Variables were measured point-to-point parallel or perpendicular to the plane of view, or parallel to feature being measured (Fig. 1 and Appendix A, Table A1). Categorical data were assessed visually and included four that were used by Charlton-Robb et al. (2011). Count data were number of teeth in each tooth row (including vestigial anterior teeth; Appendix A, Table A1) and seven vertebral counts (Appendix A, Table A1). The latter were collected only from full vertebral columns (Table 1; assessed by arranging the vertebrae in sequence), of which most (58) were from South Australia. The two small, triangular, fused, terminal caudal vertebrae were counted as one.

The 2D data were checked for outliers by visual inspection of bivariate plots and these re-measured. Data normality was assessed for each variable by examining box–whisker plots and histograms. None of the variables were skewed enough to warrant transformation. The assumption of homogeneity of variance was tested using Levene's test and assumption not violated ($P < 0.05$). Sexual dimorphism was tested using multivariate analysis of variance (MANOVA in SPSS version 20.0; IBM Corp., Armonk, New York, USA) and was visually compared using principal component analysis (PCA).

Initial multivariate analyses were performed on 218 specimens for which complete data were available. To not over-inflate the importance of size in the grouping of specimens by the analyses of the original data and to deal with potentially skewed data, cluster and discriminant function analyses were also performed on log-transformed data and principle component (PC) scores. Three analyses were performed to discriminate groups: k-means (2–3 groups in JMP), hierarchical cluster analyses (HCA; using Euclidean distance in SPSS), and discriminant function analysis (DFA; in SPSS) to confirm results from the cluster analyses. Group membership of the specimens for the DFA, as determined by the cluster analyses (defined in the Results), provided the a priori classification. In addition to these, *T. australis* specimens were assigned to a

Can. J. Zool. Downloaded from www.nrcresearchpress.com by Dr Maria Jedensjo on 06/24/20
For personal use only.

Fig. 3. Principal component analysis (PC1 vs. PC2) of bottlenose dolphin (*Tursiops* spp.) skull two-dimensional data to illustrate lack of sexual dimorphism. Only specimens with known sex are included. Colour version online.

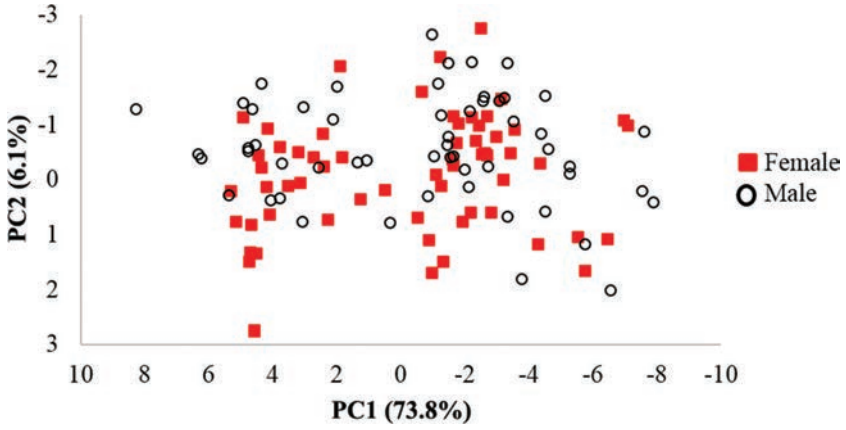

Table 2. Comparison of clustering consistency of bottlenose dolphin (*Tursiops* spp.) specimens between three 2D analyses where 0% indicates no specimens in the same group and 100% indicates all specimens in the same group.

	HCA	*k*-means	DFA
HCA	—	96.6 (n = 9)	96.6 (n = 9)
k-means	—	—	97 (n = 8)

Note: Values are percentages. For abbreviation definitions refer to Appendix A, Table A1.

separate group. To increase sample size, the data set was then re-analysed using only the most important variables (n = 25). PCA (using restricted maximum likelihood, maximum likelihood, robust, row-wise, and pairwise estimation methods in JMP) were performed to confirm groups and visualise results. MANOVA was used to test for statistically significant differences between *T. australis* and identified groups as determined by the multivariate analyses. Student's t tests and Mann–Whitney U tests were used to identify statistically significant morphological (count and categorical data: Appendix A, Table A3) differences between groups (Table 4).

Geometric morphometrics data collection and statistical protocols

A set of 73 cranial landmarks (3D point x, y, z for each landmark) was collected from 202 specimens using a 3D digitiser (MicroScribe G2X; Immersion Corporation) in dorsal and ventral planes (Fig. 2; Table 1; Appendix A, Table A4; Supplementary material S3;[1] modified from de Araujo Monteiro-Filho et al. (2002) and del Castillo et al. (2016)). Landmarks were chosen to have a good representation of the overall cranium shape that included important features. These were subjected to generalised Procrustes analysis, which scales all specimens to the same size and superimposes them by minimising the sum of squared deviations between landmark configurations. Centroid size (the square root of the sum of square distances of each landmark to its mean) was then used as proxy for the size of each individual.

After generalised Procrustes analysis, (*i*) the amount of shape variability due to sexual dimorphism, directional asymmetry, and size was quantified by means of Procrustes ANOVA. This was followed by (*ii*) assessing the presence of patterns in the data by means of hierarchical cluster analyses (HCA, Ward, and UPGMA methods) and PCA. The number of optimal clusters was chosen using the function fviz_nbcust in the package factoextra for R version 3.7.1 (Kassambara and Mundt 2017). To compare the results of the clustering with and without excluding the effect of allometry, (*iii*) HCAs were performed first on Procrustes shape data and then on the residuals from the multivariate regression between Procrustes shape coordinates and centroid size. Note that in this case, a test for inter-group differences in allometric vectors was not possible (the test for presence of distinct taxa being the aim of the paper). The use of residuals was, however, preferred to the exclusion of the first PC after addition of the centroid size to Procrustes coordinates (cf. Mitteroecker et al. 2004) to preserve as much information as possible. Finally, (*iv*) a permutational analysis of multivariate variance (PERMANOVA; 10 000 permutations) was used to test for statistically significant differences between the clusters identified in step *iii*.

Geometric morphometric analyses were carried out in MorphoJ version 1.06 (Klingenberg 2011), PAST version 3.14 (Hammer et al. 2001), and R version 3.3.1 (R Core Team 2016), using the packages MASS, Morpho, vegan, factoextra, and geomorph (respectively, Venables and Ripley 2002; Schlager 2017; Oksanen et al. 2018; Kassambara and Mundt 2017; Adams et al. 2018). Visualisation of shape changes was obtained by warping a wireframe representation of a generic *Tursiops* cranium via a thin-plate-spline (TPS) algorithm in Morphologika version 2.5.

Geographical analyses

Correlations between cranial shape (3DGM Procrustes residuals data) and geographic distances were tested using a Mantel test in the R package ecodist (Goslee and Urban 2007). Pearson's correlation coefficients and 95% confidence intervals (n bootstraps = 1000) were obtained and assessed for statistical significance using 10 000 permutations. The 3DGM Procrustes data were first transformed into Procrustes residuals data that were converted into a pairwise matrix (Euclidean index setting) using PAST version 3.14 (Hammer et al. 2001). Geographic distances between specimens were calculated as dyadic least-cost path distances using the gdistance package (van Etten 2015) in R version 3.3.1 (R Core Team 2016). Distance matrices were defined such that only travel through oceanic water was possible (at a uniform cost), with shorelines demarcated by the SRTM Water Bodies data set (Environmental Systems Research Institute, Inc. 2008), projected in the Geocentric Datum for Australia (GDA94) at a raster resolution of 10 km.

Results

Two-dimensional, count, and categorical data

No sexual dimorphism was detected in the 2D measurements (MANOVA, $F_{[76,268]} = 1.303$, $P < 0.05$, female = 51, male = 55; PCA in Fig. 3); therefore, sexes were combined in all subsequent analyses.

The *k*-means and HCA on the original, log-transformed, and PC score data separated most specimens into two groups (2D-1 and 2D-2) and their assignment was the same for all tests (only results using original data are presented in the Results, as log-

Can. J. Zool. Downloaded from www.nrcresearchpress.com by Dr Maria Jedensjo on 06/24/20
For personal use only.

Fig. 4. Principal component analysis (PC1 vs. PC2) of bottlenose dolphin (*Tursiops* spp.) skull two-dimensional data. (A) Results from the present study, (B) a visual comparison with species identification by Charlton-Robb et al. (2011), and (C) a visual comparison with species identification by Kemper (2004). *Da*, *Delphinus aduncus* holotype (BZM 66400); *Dt*, *Delphinus truncatus* holotype (NHMUK 353a); *Tau*, *Tursiops australis* paralectotype (QVM 1365); *Tm*, *Tursiops maugeanus* junior synonym of *Tursiops truncatus* (QVM 1360); *Dc*, *Delphinus catalania* syntype (NHMUK 1862.6.6.13).

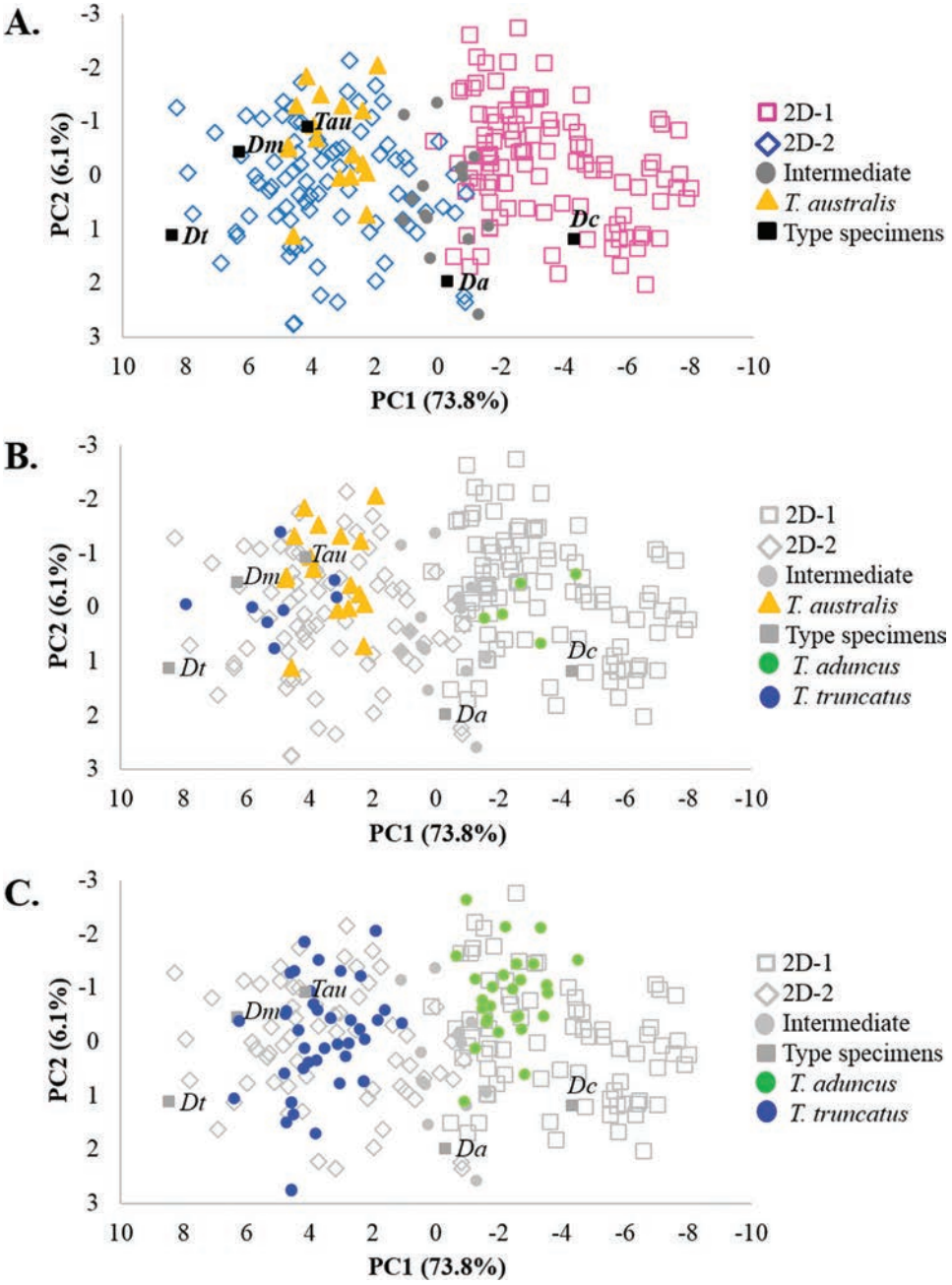

transformed and PC scores did not improve the outcome). No sexual dimorphism was detected when testing within each group (MANOVA, 2D-1: $F_{[16,72]} = 1.347$, $P < 0.05$; MANOVA, 2D-2: $F_{[9,42]} = 2.00$, $P < 0.05$). Specimens identified as *T. australis* were well embedded in *T. truncatus* for both analyses. Thirteen specimens aligned with different groups in the tests (Table 2) and are here defined as intermediate (see Supplementary material S1).[1]

PCA is a useful way to visualise the data in 2D space because it illustrates the relationship of the groups and intermediates (Fig. 4A). Note the overlap between 2D-1 and 2D-2. A comparison was also made for the 44 specimens examined by Charlton-Robb et al. (2011), and used for their hierarchical multivariate cluster analyses, where all 5 *T. aduncus*, 8 of 13 *T. truncatus*, and 21 of 26 *T. australis* specimens were used in the present study (Fig. 4B). The same comparison was also made for the 84 specimens examined by Kemper (2004), where 27 of 59 *T. aduncus* and 22 of 25 *T. truncatus* specimens were used in the present study (Fig. 4C). Thus, it appears that 2D-1 represents *T. aduncus* and 2D-2 represents *T. truncatus*. Importantly, *T. australis* specimens fell entirely within the *T. truncatus* cluster (Figs. 4A–4C).

A similar pattern was apparent when many variables (e.g., GPOW; Fig. 5) were plotted against CBL, in this case showing the importance of skull size in discriminating groups. The *T. aduncus* group contained small skulls, including the type specimen

Can. J. Zool. Downloaded from www.nrcresearchpress.com by Dr Maria Jedensjo on 06/24/20
For personal use only.

Fig. 5. Plot of CBL vs. GPOW showing size variation between bottlenose dolphins *Tursiops aduncus*, *Tursiops truncatus*, and 2D intermediate groups. Group clustering based on HCA and DFA results. *Da*, *Delphinus aduncus* holotype; *Dt*, *Delphinus truncatus* holotype; *Tau*, *Tursiops australis* paralectotype; *Tm*, *Tursiops maugeanus* junior synonym of *T. truncatus*; *Dc*, *Delphinus catalania* syntype. For other abbreviation definitions see Appendix A, Tables A1 and A2.

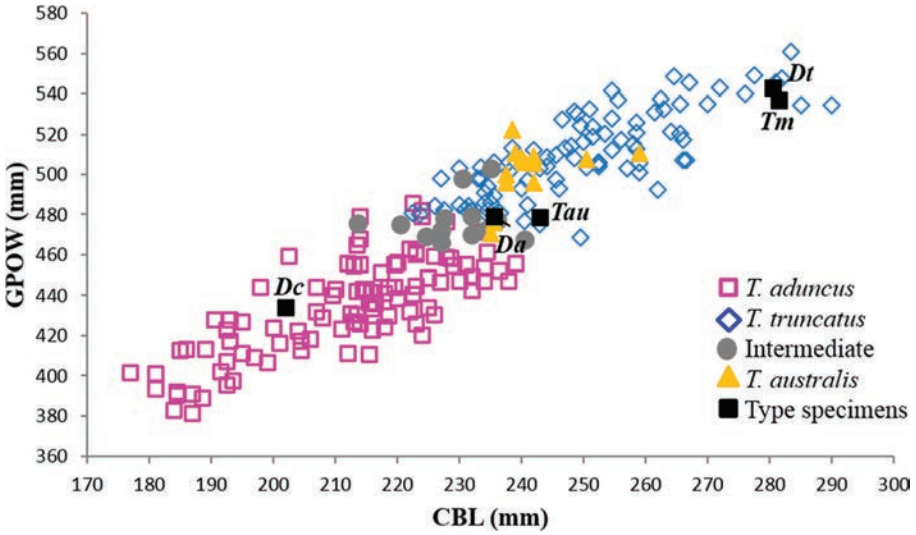

Table 3. Bottlenose dolphin (*Tursiops* spp.) 2D variables with PCA loadings for the first four PCs (varimax rotation).

Variable	PC1	PC2	PC3	PC4
Length				
CBL: condylobasal length	0.589	*0.724*	0.269	0.145
RL: rostrum length	0.455	*0.817*	0.236	0.158
TREN: tip of rostrum to external nares	0.470	*0.786*	0.241	0.147
ILB: internal length of braincase	*0.734*	0.421	0.300	0.121
TRPS: tip of rostrum to medial palatine suture	0.496	*0.786*	0.257	0.089
UTLTR: length of upper tooth row to tip of rostrum	0.452	*0.792*	0.218	0.135
ML: mandible length	0.577	*0.749*	0.247	0.120
LTRL: length of lower tooth row to tip of rostrum	0.454	*0.800*	0.206	0.127
MSL: mandibular symphysis length	0.202	*0.744*	0.125	0.128
Width				
RW60: rostrum width at 60 mm from base	*0.760*	0.507	0.221	0.183
RW75%: rostrum width at 3/4 of rostrum length	*0.765*	0.416	0.162	0.159
RWM: rostrum width at mid-length	*0.780*	0.459	0.245	0.171
RW25%: rostrum width at 1/4 of rostrum length	*0.754*	0.447	0.211	0.186
PRW: premaxillae width at mid-rostral length	*0.756*	0.343	0.374	0.122
WRN: greatest width of right nasal	0.329	0.237	*0.738*	0.169
WLN: greatest width of left nasal	0.244	0.211	*0.809*	0.141
ZW: zygomatic width	*0.728*	0.479	0.186	0.415
GPOW: greatest postorbital width of skull	*0.760*	0.519	0.251	0.189
GPARW: greatest width across parietals	*0.811*	0.182	0.330	0.127
GWPTF: greatest width of left temporal fossa	*0.746*	0.251	0.204	0.165
WAS: width of alisphenoid at suture with the basisphenoid	*0.738*	0.543	0.195	0.185
Height				
HRN: greatest height of right nasal	0.104	0.054	0.207	*0.849*
EHB: external height of braincase	*0.784*	0.444	0.326	0.154
EHBHP: external height of braincase to highest point	*0.765*	0.494	0.292	0.183
MH: mandible height	*0.712*	0.549	0.288	0.093
PC eigenvalue	29.32	1.82	1.47	1.18
Total variance (%)	68.7	4.7	3.5	2.8
Cumulative variance (%)	68.7	73.4	76.9	79.7

Note: Variables with PCA loadings >0.7 for one or more PCs are shown in italic type. For abbreviation definitions refer to Appendix A, Table A1.

D. catalania, while the type specimen *D. aduncus* fell between the two groups. The *T. truncatus* group contained large skulls, including the type specimens *D. truncatus*, *T. australis*, and *T. maugeanus*, as well as all *T. australis* specimens (Figs. 4A–4C and 5).

Each of the first four PCs had eigenvalues greater than 1 and were therefore useful in discriminating the components. These PCs accounted for 79.7% of the total variance, with PC1 alone accounting for 68.7% (Table 3). Width variables contributed most

Can. J. Zool. Downloaded from www.nrcresearchpress.com by Dr Maria Jedensjo on 06/24/20
For personal use only.

Table 4. Count and categorical variables showing significant differences between specimens of bottlenose dolphins *Tursiops aduncus* and *Tursiops truncatus*.

	T. aduncus			*T. truncatus*					
Variable	*n*	Range	Mean	*n*	Range	Mean	*t* or *U*	df	*P*
Count									
TLL	101	19–29	24.32	83	19–29	23.68	2.66	182	<0.01
TLR	98	19–29	24.18	82	20–29	23.63	2.20	178	<0.01
TD	86	4.7–8.2	5.79	73	5.6–7.9	6.70	11.05	157	<0.001
TV	56	11–13	11.91	31	12–13	12.19	3.45	85	<0.001
XV	56	11–17	14.75	29	12–19	16.00	3.93	83	<0.001
YV	53	15–20	17.28	29	17–21	19.14	7.65	80	<0.001
Z	45	6–10	8.36	22	7–10	8.86	2.39	56	<0.05
TOTV	42	57–62	59.28	16	61–65	63.00	7.82	66	<0.001
VPVF	55	31–47	39.38	29	40–46	44.31	8.30	82	<0.001
Categorical									
Resorption to pterygoid	109	1–4	2	100	1–4	2	3145		<0.001
Extent of nuchal crest	118	1–4	2	115	1–3	2	4048		<0.001
Highest point of skull	119	1–4	2	114	1–4	2	4779		<0.001
Pterygoid and palatine length	109	1–3	1	100	1–3	1	4546		<0.05
Arch of premaxilla	119	1–3	1	115	1–3	1	5819		<0.05

Note: Significance level (*P*) for the Student's *t* test (count data) and Mann–Whitney *U* test (categorical data) are provided. None statistically significant categorical and count data included temporal fossa shape, pterygoid hamular ridge shape, position of lower tip of pterygoid versus top maxilla suture, pterygoid to maxilla suture, palatine shape, teeth upper left and right, and cervical vertebrae. For abbreviation definitions refer to Appendix A, Tables A1, A2, and A3.

Table 5. Bottlenose dolphin (*Tursiops* spp.) 3DGM results of Procrustes ANOVA showing (A) effects of sex and directional asymmetry on size on shape variance and (B) effect of size on shape variance.

Effect	SS	MS	df	*F*	*P*	R^2
(A) Sex and directional asymmetry on size on shape variance.						
Centroid size						
Sex	357.346	357.346	1	0.04	0.843	
Individual	1 036 419.118	9 091.396	114			
Shape						
Sex	0.00168	0.0000210	80	0.86	0.805	
Individual	0.223	0.0000244	9 120	8.58	<0.001	
Side	0.0346	0.000461	75	161.99	<0.001	
Residuals	0.0245	0.00000284	8 625			
(B) Size on shape variance.						
Centroid size	0.0723	0.0723	1	37.409	<0.001	0.158
Residuals	0.387	0.00193	200			0.842
Total	0.460		201			

Note: All analyses included 10 000 permutations. For abbreviation definitions refer to Appendix A, Table A1.

to the variance in PC1 and three height and one length variable also being important (Table 3). For PC2, only length variables had PC loadings greater than 0.7 (Table 3).

A DFA was carried out on three groups, representing *T. aduncus*, *T. truncatus* (as defined by the cluster analyses), and *T. australis* (Figs. 4A–4C; Charlton-Robb et al. 2011), followed by MANOVA. The first discriminant function was statistically significant (Wilks' λ = 0.139, $P < 0.001$) and loaded on the following variables: CBL, GPOW, ZW, UTLTR, ML, MH, and GWPTF. The discriminant functions provided correct classification for all *T. aduncus* (100%) and *T. truncatus* (100%) specimens when testing for two groups. When *T. australis* specimens were classified as a separate group, they were classified with 68.2% accuracy, whereas *T. aduncus* and *T. truncatus* were classified with 100% and 93.6% accuracy, respectively. In addition, the MANOVA results ($F_{[76,268]} = 1.205$, $P < 0.001$) supported *T. aduncus* and *T. truncatus* as separate groups, whereas *T. australis* specimens could not be distinguished from *T. truncatus* for any data used (original, log-transformed, or PC scores; $P > 0.05$).

Comparison of count and categorical data for *T. aduncus* and *T. truncatus* specimens resulted in statistically significant differences for some variables (Table 4). Compared with *T. truncatus* specimens, *T. aduncus* had more teeth in the lower tooth rows; smaller tooth diameter; more erosion to the pterygoids (possibly parasite related); a lower, nuchal crest at the highest point of the skull; pterygoid and palatine of unequal length; flatter arch of the premaxilla; and fewer vertebrae. *Tursiops australis* specimens were not significantly different from *T. truncatus* for any of the count or categorical data, including those used by Charlton-Robb et al. (2011).

Geometric morphometrics

Procrustes ANOVA (Tables 5A and 5B) revealed a significant effect of directional asymmetry and size on the shape variance of the specimens. Conversely, no significant effect was found for sex. Therefore, the analyses below used only the asymmetric component of variation and combined females and males.

Cluster analyses using Ward and UPGMA on PC of original shape data (Figs. 6A and 6B; 73 landmarks) showed similar assignment when specimens fell into two groups (3DGM-1 and 3DGM-2). Group 3DGM-1 included type specimens of *D. aduncus* and *D. catalania*, while 3DGM-2 included type specimens of *D. truncatus*, *T. maugeanus*, and *T. australis*, as well as non-type *T. australis*. However, the *T. australis* type specimen did not cluster together with other *T. australis* for UPGMA, but it did for Ward (Figs. 6A and 6B).

Can. J. Zool. Downloaded from www.nrcresearchpress.com by Dr Maria Jedensjo on 06/24/20
For personal use only.

Can. J. Zool. Downloaded from www.nrcresearchpress.com by Dr Maria Jedensjo on 06/24/20
For personal use only.

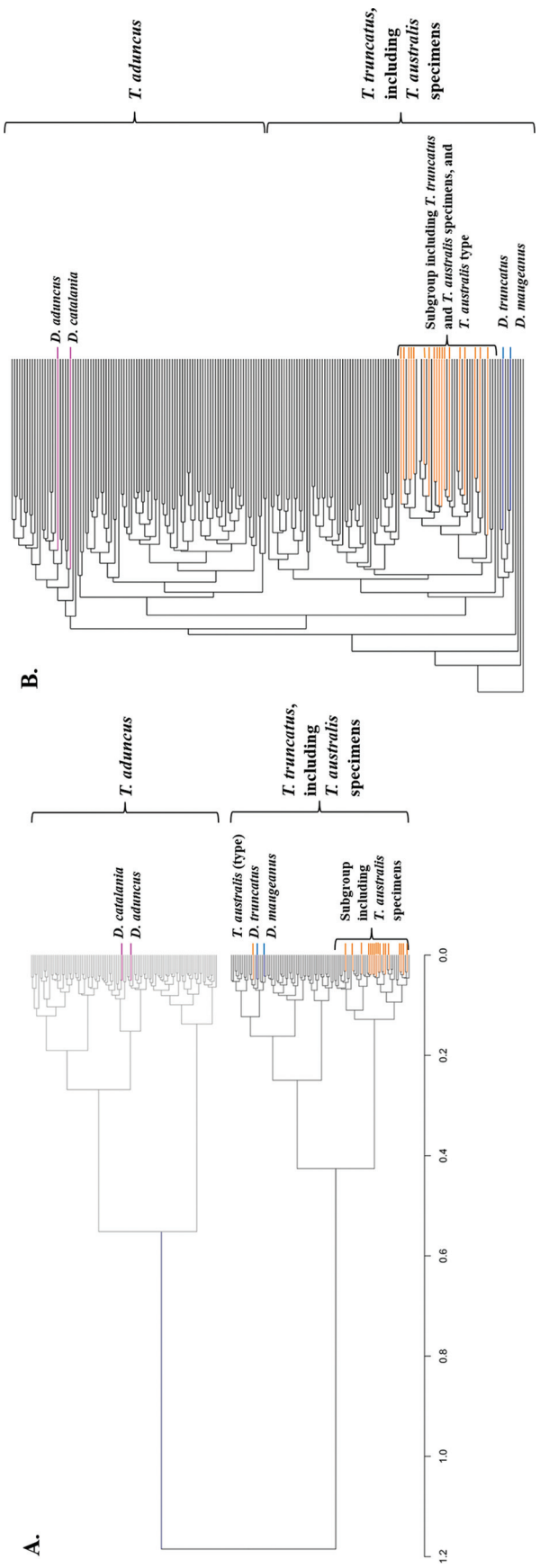

Fig. 6. HCA results (Procrustes shape data using 73 landmarks) for 3DGM, including all Australian bottlenose dolphins (*Tursiops* spp.) and type specimens. (A) Ward and (B) UPGMA. The positions of the five type specimens (original names) and Burrunan dolphin (*Tursiops australis*) specimens are shown. For abbreviation definitions see Appendix A, Table A1. Colour version online.

PERMANOVA confirmed a statistical difference between the two groups (F = 39.349, P < 0.001; Table 6). A boxplot of centroid size between 3DGM-1 and 3DGM-2 showed the marked smaller size of the individuals in 3DGM-1 (Fig. 7) and the overlapping size of *T. australis* and other specimens in 3DGM-2. When 3DGM-1 and 3DGM-2 were themselves divided into two subgroups, these were significantly different from each other (F = 26.46, Bonferroni-corrected P < 0.001). However, the subgroup composition of these clusters varied slightly between Ward and UPGMA, where 18% (n = 37) of the specimens were assigned to different subclusters. These subgroups showed some geographical separation, where one of the 3DGM-1 subgroups contained more samples from northern Australia, while the other one contained more samples from southern Australia. One of the 3DGM-2 subgroups contained *T. australis* specimens and other specimens from southern parts of Australia (Figs. 6A and 6B), while the other subgroup contained specimens from both southern and northern parts.

To ensure the 73 landmarks were representative, the same cluster analyses (Ward and UPGMA) were also performed on the PC of original shape data using 54 landmarks (removing landmarks 3, 4, 7–10, 24, 26, 37, 38, 40–42, 44, 53, 63, 65, 68 and 70; Fig. 2). The results showed the same two groupings and group assignments for each specimens as analyses above (Supplementary material S4).[1]

The second set of HCAs (performed on the residuals of shape vs. centroid size on 54 landmarks) also resulted in two groups for both Ward and UPGMA (Figs. 8A and 8B) that were significantly different (PERMANOVA, F = 24.53, P < 0.001; Table 6). Of note is that group composition of these clusters was very different from that of the first set of HCAs on the original shape data. Firstly, one of the groups only contained 37 specimens and the second contained 165 specimens. Secondly, about half of the specimens (n = 63; 86% of the specimens) changed group assignment (Figs. 6A, 6B, 8A, and 8B; Tables 7A and 7B), a result which is consistent with the importance of allometry in the shape variability of our specimens. *Tursiops australis* specimens fell within the same group, as did the type specimens *D. truncatus*, *T. australis*, and *T. maugeanus* for both HCAs. A counter-intuitive result was the position of *D. aduncus* (UPGMA) and *D. catalania* (Ward) because they were not associated together. The *T. australis* type specimen did not cluster together with other *T. australis* for Ward, but it did for UPGMA (Figs. 6A and 6B), which is reverse of the analyses using the original shape data.

When the two groups (3DGM-1 and 3DGM-2) were themselves divided into two subgroups, these were significantly different from each other (Ward: F = 20.61, Bonferroni-corrected P < 0.001). The *T. australis* specimens clustered in one of the subgroups with other *T. truncatus* specimens, but without the *T. australis* type for UPGMA (Figs. 6A and 6B).

A PCA plot of the 3DGM results (on the original coordinate configurations) with specimens labelled according to the 2D species identification (Fig. 9 and Table 7) showed that 3DGM-1 and 3DGM-2 appear to largely represent *T. aduncus* and *T. truncatus*. Only 10 specimens had different subgroup assignments, while almost half of the specimens fell into different groups when comparing 2D results to the second HCA (size-corrected data). This confirmed that the difference between the two groups (including, respectively, *T. aduncus* and *T. truncatus*) was largely due to allometry, which are summarised by the distribution of the sample along the first PC of 2D data (correlation with size: 0.9). In addition, the 2D results showed more overlap in subgroups in the Ward analysis compared with UPGMA. Eight of the 2D intermediate specimens clustered with *T. aduncus* for the 3DGM and four clustered with *T. truncatus* (Fig. 9 and Table 7). Three-dimensional shape changes differentiating *T. aduncus* and *T. truncatus* included a more rounded cranium in *T. aduncus* and a more angular cranium in *T. truncatus* (Fig. 10). The *T. aduncus* specimens had a longer and narrower rostrum than the *T. truncatus* specimens. Other differences were related to the supraoccipital, basioccipital, apex of

Table 6. Bottlenose dolphin (*Tursiops* spp.) 3DGM results of PERMANOVA (10 000 permutations) of size-uncorrected and size-corrected shape data with clustering as factor.

Effect	SS	MS	df	*F*	*P*
Size-uncorrected data					
Clustering (two clusters)	0.07711	0.07711	1	39.349	<0.001
Size-corrected data					
Clustering (two clusters)	0.04088	0.040875	1	24.53	<0.001

Note: For abbreviation definitions refer to Appendix A, Table A1.

Fig. 7. Boxplot of centroid size for Australian bottlenose dolphins (*Tursiops* spp.) showing size variation between groups 3DGM-1, 3DGM-2, and Burrunan dolphin (*Tursiops australis*). Group clustering based on results from HCA. Box limits indicate the 25th (lower) and 75th (upper) quartiles; the solid line within the box indicates the mean; whiskers indicate the last datum within 1.5 interquartile ranges of the box limits. For abbreviation definitions see Appendix A, Table A1.

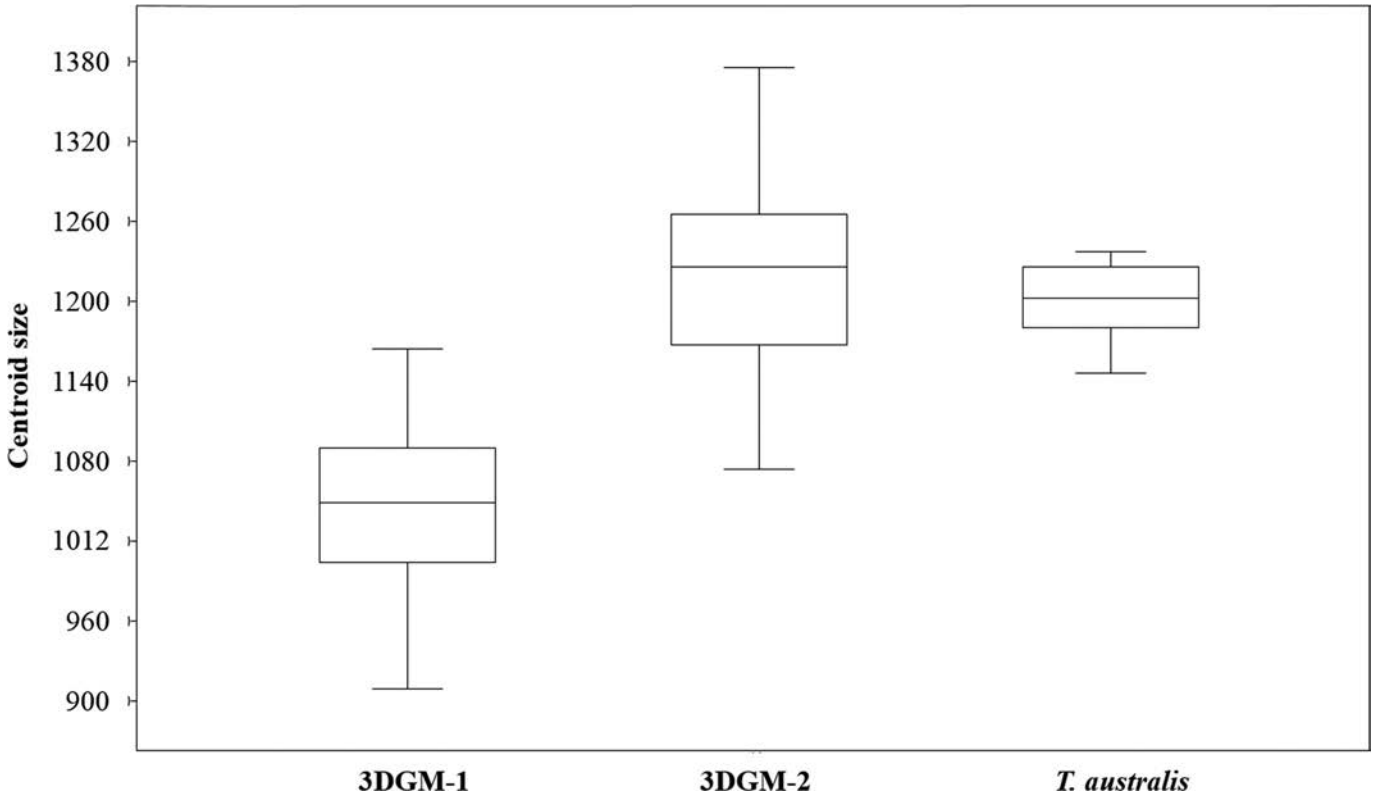

Can. J. Zool. Downloaded from www.nrcresearchpress.com by Dr Maria Jedensjo on 06/24/20
For personal use only.

the premaxillary convexity, external nares, temporal fossa, pterygoids, and lacrimojugal as shown in Figs. 8A and 8B.

Geographical trends

With one exception, specimens from the Northern Territory aligned with *T. aduncus*, whereas those from Victoria and Tasmania aligned with *T. truncatus* (Fig. 11). The 2D intermediate specimens came from around the coast of Australia. Queensland, New South Wales, South Australia, and Western Australia had specimens from both morphological groups. This trend was confirmed when latitude and CBL were compared for *T. aduncus* specimens (Fig. 12). There were no latitudinal trends for *T. truncatus* specimens.

Specimens were morphologically more different with increasing dyadic geographical distance using Procrustes data (*T. aduncus*: Pearson's $r = 0.390$, 95% bootstrapped CI = 0.352–0.435, P permutation < 0.001; *T. truncauts*: Pearson's $r = 0.281$, 95% bootstrapped CI = 0.243–0.316, P permutation < 0.001).

Discussion

The results of the present study support for the presence of two species of bottlenose dolphin in Australia: *T. aduncus* and *T. truncatus*. The holotypes of these species were larger than their Australian conspecifics and fell at the periphery of the 2D PC clusters. The Australian type specimens of *T. australis*, *T. maugeanus*, and *D. catalania* aligned better with their respective species.

Charlton-Robb et al. (2011) concluded that *T. australis* could be distinguished from *T. aduncus* and *T. truncatus* using four diagnostic skull features and that its size was intermediate. Their study was based on few specimens from widely spaced regions and they did not compare with morphological results for South Australian bottlenose dolphins (Kemper 2004). Our previous morphological results for the genus *Tursiops* in Australian waters found a clear separation between *Tursiops* spp. from other genera and *T. australis* clustering together with *T. aduncus* and *T. truncatus* (Jedensjö et al. 2017). In addition, the present study could not distinguish *T. australis* from *T. truncatus*, including for the characteristics used by Charlton-Robb et al. (2011). Interestingly, the *T. australis* type specimen did not cluster with other *T. australis* specimens for several analyses, suggesting that it may not be an appropriate choice to represent *T. australis*.

Intermediately sized skulls were identified in the present study using 2D analyses, but they did not align with the *T. australis* specimens studied by Charlton-Robb et al. (2011). Overlap in skull size of *T. aduncus* and *T. truncatus* has previously been identified in South Australia (Kemper 2004) and South Africa (Ross 1977), but

Can. J. Zool. Downloaded from www.nrcresearchpress.com by Dr Maria Jedensjo on 06/24/20
For personal use only.

Fig. 8. HCA results (performed on the residuals of shape vs. centroid size on 54 landmarks) for 3DGM, including all Australian bottlenose dolphins (*Tursiops* spp.) and type specimens. (A) Ward and (B) UPGMA. The positions of the five type specimens (original names) and Burrunan dolphin (*Tursiops australis*) specimens are shown. For abbreviation definitions see Appendix A, Table A1. Colour version online.

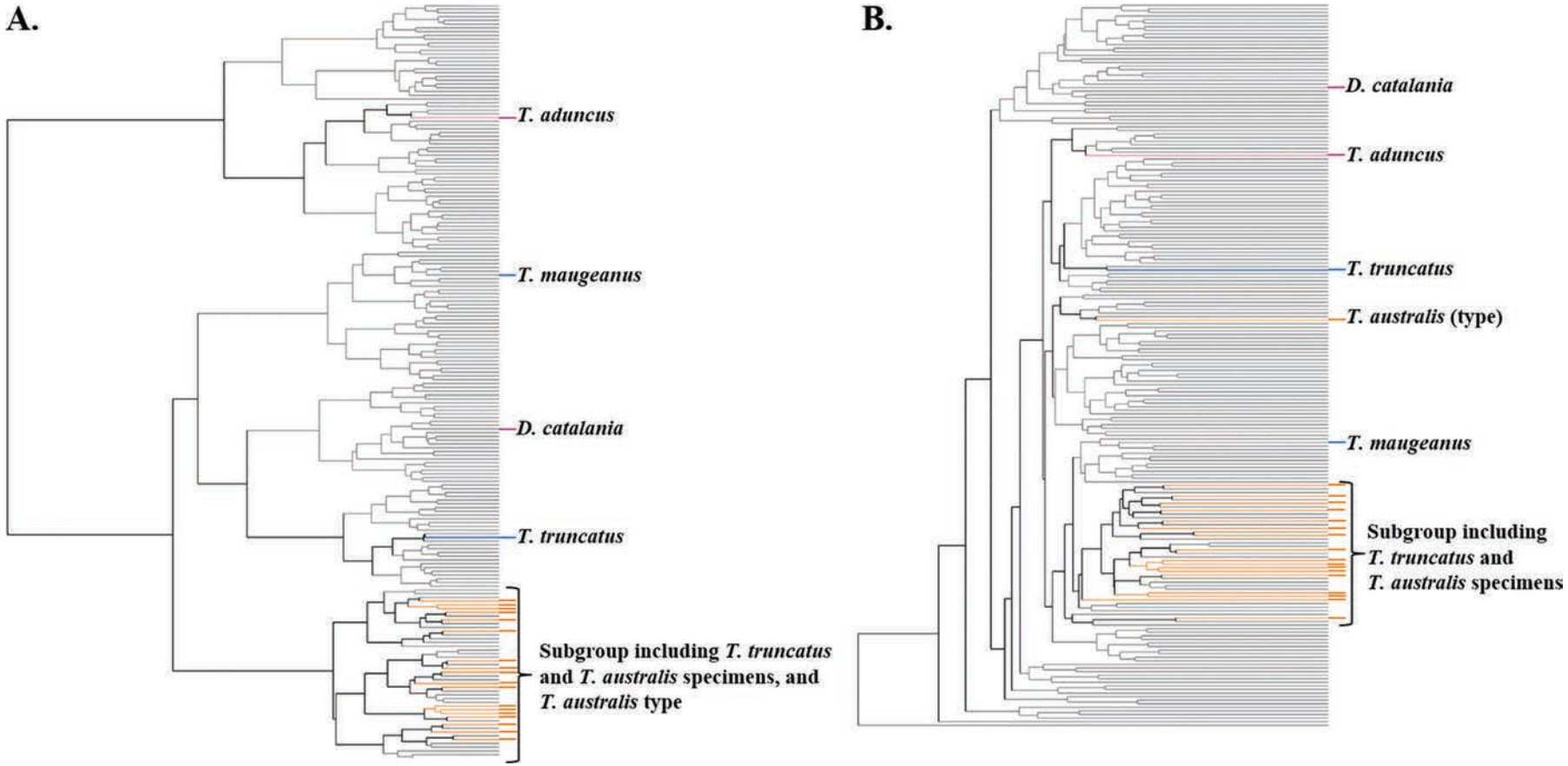

Can. J. Zool. Downloaded from www.nrcresearchpress.com by Dr Maria Jedensjo on 06/24/20
For personal use only.

Table 7. Bottlenose dolphin (*Tursiops* spp.) specimens (1, *Tursiops aduncus*; 2, *Tursiops truncatus*) with discordant clustering groups for (A) the two 3DGM cluster analyses (original coordinate configurations and shape data) and the 2D results and (B) geometric morphometric clustering groups for the 2D intermediate specimens (inter).

ID	Sampling location	2D	3DGM (original)	3DGM (shape)
(A) Specimens with discordant clustering groups for 2D results.				
Percy Island	QLD	2	1	1
QMJM10114	QLD	1	2	2
M10852	NSW	1	2	2
M22971	NSW	2	1	2
M20878	SA	1	2	2
M19952	SA	1	2	2
M18048	SA	1	1	2
M24726	SA	2	1	2
M4794	WA	2	1	1
M7871	WA	2	1	1
Three of the specimens	NSW, SA	2	2	1
Seventy of the specimens	All	1	1	2
Tursiops catalania (type)	QLD	1	1	2
Tursiops aduncus (type)	Red Sea	1	1	2 (UPGMA)
(B) 2D intermediate specimens.				
M5723	WA	Inter	1	2
M7499	WA	Inter	1	1
M7584	WA	Inter	1	2
M15245	WA	Inter	1	2
M16298	WA	Inter	1	1
M25813	WA	Inter	1	1
M22838	NSW	Inter	1	2
Unregistered	TAS	Inter	1	2
C24990	VIC	Inter	1	2
M5902	SA	Inter	2	2
U0534	NT	Inter	2	2
JM7015	QLD	Inter	2	2

Note: For abbreviation definitions refer to Appendix A, Table A1.

Fig. 9. Plot of PC1 vs. PC2 for 3DGM data including all bottlenose dolphins (*Tursiops* spp.). Specimens labelled according to results of the 2D multivariate analysis. *Da*, *Delphinus aduncus* holotype (BZM 66400); *Dt*, *Delphinus truncatus* holotype (NHMUK 353a); *Tau*, *Tursiops australis* paralectotype (QVM 1365); *Tm*, *Tursiops maugeanus* junior synonym of *Tursiops truncatus* (QVM 1360); *Dc*, *Delphinus catalania* syntype (NHMUK 1862.6.6.13). For abbreviation definitions see Appendix A, Table A1.

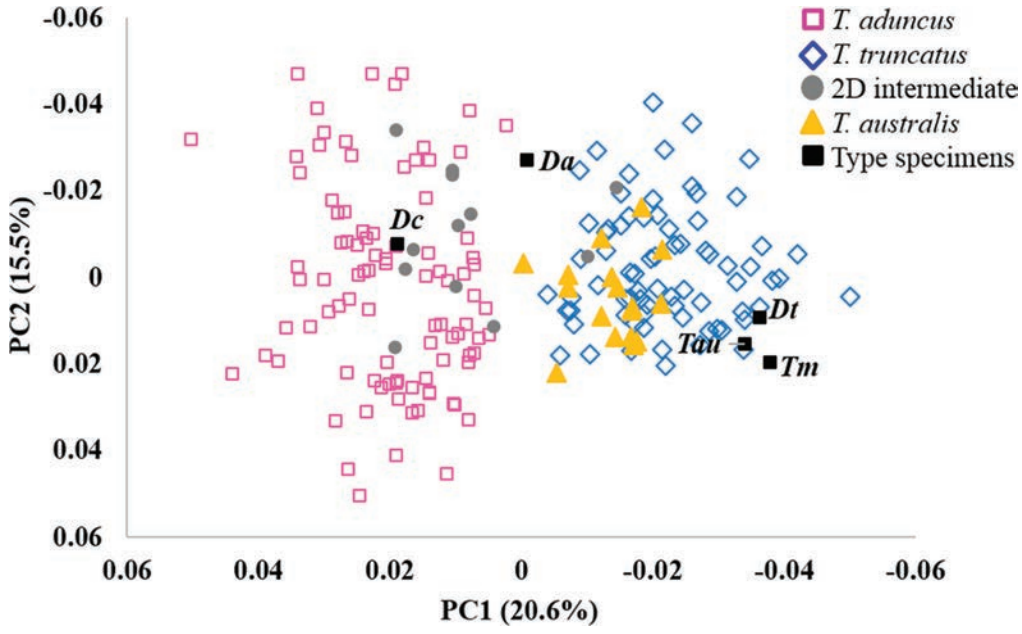

Can. J. Zool. Downloaded from www.nrcresearchpress.com by Dr Maria Jedensjo on 06/24/20
For personal use only.

Fig. 10. Dorsal, lateral, ventral, and posterior views of bottlenose dolphin (*Tursiops* spp.) cranium for 3DGM *Tursiops aduncus* and *Tursiops truncatus* specimens along PC1 axis. (Left) Example of an extreme *T. aduncus*, and photographs of holotype *Delphinus aduncus* (BZM66400), and syntype of *Delphinus catalania* (1862.6.6.13). (Right) Example of an extreme *T. truncatus*, and photographs of holotype *Delphinus truncatus* (353a), and type specimen of *Tursiops australis* (1365). Posterior and ventral images show the PC1 angular vs. round-shaped difference between *T. aduncus* and *T. truncatus* specimens. (1*a*, 1*b*) Rostrum length and width; (2*a*, 2*b*) posterior flange of temporal fossa; (3*a*, 3*b*) apex of premaxillary convexity; (4*a*, 4*b*) position of external nares; (5*a*, 5*b*) supraoccipital shape; (6*a*, 6*b*) pterygoid shape and position; (7*a*, 7*b*) preorbital (lacrimojugal) position; (8*a*, 8*b*) width of alisphenoid at the suture with basisphenoid; (9*a*, 9*b*) distance between nuchal crest and occipital condyles; (10*a*, 10*b*) length of temporal fossa; (11*a*, 11*b*) nuchal crest shape; (12*a*, 12*b*) distance between landmark 34 (zygomatic width) and landmark 73 (paraoccipital process). For abbreviation definitions see Appendix A, Table A1. Colour version online.

Fig. 11. Geographic distribution of Australian bottlenose dolphins (*Tursiops* spp.): *Tursiops aduncus* (squares), *Tursiops truncates* (diamonds), and intermediate (circles). Groups are as determined by multivariate analyses. Figure was created using ArcGIS version 10.1 using base map GEODATA COAST 100K 2004 (shapefiles; Geoscience Australia 2004).

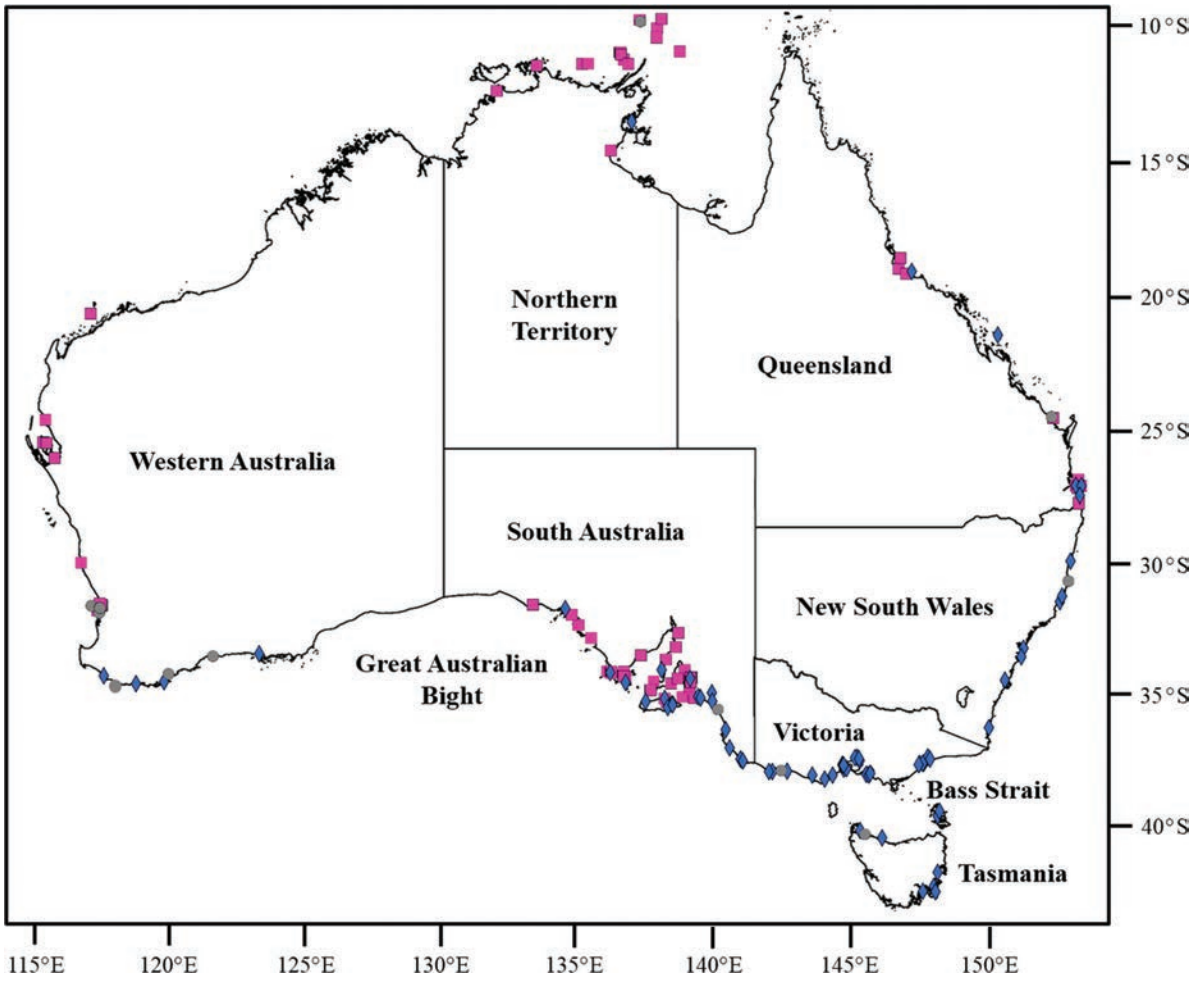

Fig. 12. Condylobasal length (CBL) plotted against latitude for *Tursiops aduncus* specimens of known location as determined by two-dimensional multivariate analyses. No *Tursiops aduncus* specimens were available from Victoria or Tasmania. For abbreviation definitions see Appendix A, Table A1. Colour version online.

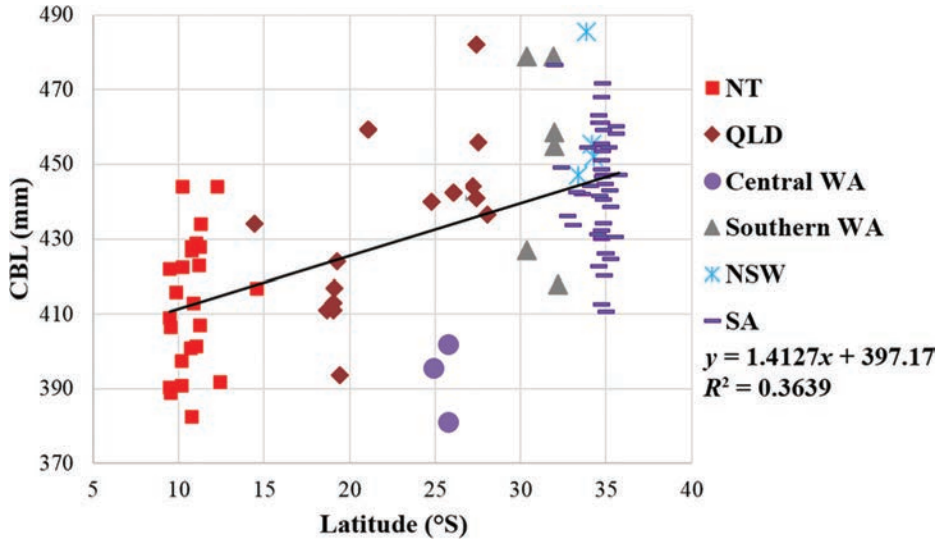

Can. J. Zool. Downloaded from www.nrcresearchpress.com by Dr Maria Jedensjo on 06/24/20
For personal use only.

Table 8. Comparison of osteological variables (minimum–maximum; mm) of bottlenose dolphin (*Tursiops* spp.) skull measurements between species found in Australia (present study, based on 2D results), China (Wang et al. 2000*b*), Japan (Kurihara and Oda 2007), and South Africa (Ross 1977, 1984).

	Tursiops aduncus				*Tursiops truncatus*					
Variable	China	South Africa	Japan	Australia	China	South Africa	Japan	Australia	*Tursiops australis* (Victoria, Tasmania)	Intermediate (Australia)
CBL	451–529 18, 485, 22	433–507 33, 473, 16	480–501 5, 492, 9	381–486 99, 434, 24	394–561 50, 506, 33	504–578 9, 546, 26	477–554 19, 513, 20	469–561 85, 510, 22	471–523 17, 501, 13	466–503 13, 477, 11
ML	386–461 17, 415, 21	373–422 30, 400, 15	404–429 3, 416, 0.1	312–421 91, 366, 22	341–481 51, 434, 30	426–498 9, 466, 27	395–489 19, 441, 0.3	401–475 60, 440, 20	405–449 21, 427, 12	393–419 8, 402, 9
RL	258–317 18, 282, 15	250–297 33, 272, 12	273–300 5, 288, 0.1	212–282 99, 242, 15	204–320 49, 284, 23	283–335 9, 309, 18	255–317 19, 284, 0.2	260–315 85, 289, 13	264–297 18, 278, 9	256–290 13, 270, 10
ZW	209–251 13, 231, 14	198–251 30, 230, 11	214–248 5, 234, 0.2	176–244 98, 211, 15	189–290 50, 257, 21	257–313 9, 282, 20	226–299 19, 258, 0.4	221–292 84, 253, 17	235–256 21, 243, 5	214–241 13, 231, 7
MH	77–93 17, 83, 4	72–90 30, 83, 4	79–95 3, 85, 0.1	62–89 91, 77, 6	61–104 51, 91, 8	90–110 9, 100, 6	81–110 19, 94, 0.2	80–107 60, 92, 5	84–96 21, 89, 3	79–88 8, 85, 3
RWM	56–71 18, 64, 5	56–75 32, 65, 4	60–73 5, 68, 0.1	45–73 99, 61, 6	55–102 46, 84, 9	73–106 9, 89, 11	71–105 19, 86, 0.2	61–101 85, 80, 8	70–84 18, 79, 4	63–76 13, 68, 4
Teeth total	96–111 19, 102, 4	97–111 29, 103, 4	NA NA	82–114 86, 98, 5	80–106 54, 94, 5	88–96 9, 93, 2	NA NA	81–109 54, 97, 6	93–115 19, 101, 6	96–108 8, 101, 4
Vertebrae	59–62 19, 60, 1	59–62 9, 61, 1	NA NA	57–62 42, 59, 9	64–67 20, 66, 1	64–65 4, 65, 1	NA NA	61–65 16, 63, 1	63–64 3, 63, 1	58 1, 58, NA

Note: Included are *T. aduncus*, *T. truncatus*, *T. australis* (Charlton-Robb et al. 2011), and 13 intermediate specimens from 2D multivariate analyses. The row below the range for each variable shows the total number, mean, SD, and not available (NA), respectively. For abbreviation definitions refer to Appendix A, Tables A1 and A2.

Can. J. Zool. Downloaded from www.nrcresearchpress.com by Dr Maria Jedensjo on 06/24/20
For personal use only.

not in Chinese waters (Wang et al. 2000*b*). The matter of intermediates is an interesting one and requires more study.

One of the strengths of the present study was the comparison of 2D and 3D methods for the same specimens. This enabled an examination of the effect of allometric patterns on shape variability. Although size standardisation is also possible for 2D data (e.g., by dividing all measurements by the length of the skull), very few 3DGM studies have been published for *Tursiops* spp. When not controlling for size, 2D and 3DGM analyses showed many similarities in species composition. However, for size-corrected 3DGM results, *T. aduncus* and *T. truncatus* specimens were not separated into two distinct groups, which suggests that shape differences are mostly due to size. *Tursiops australis* specimens aligned with *T. truncatus* for both 2D and 3DGM data if size was included or excluded from the analyses. *Tursiops australis* specimens clustered in a subgroup together with other *T. truncatus* specimens from southern Australia for all 3DGM analyses.

Primary drivers for adaptation in cetaceans include feeding (Heyning and Mead 1996), sound production (Mead 2009), and swimming (Long et al. 1997). For example, rostrum shape and length and the number of teeth are related to prey size (Rice 1998; Rommel et al. 2009). For bottlenose dolphins (Ross 1977; Wang et al. 2000*b*; Kurihara and Oda 2007; present study), *T. aduncus* had a longer and narrower rostrum and more teeth than *T. truncatus*. This implies a difference in diet and habitat, which has been demonstrated for South Australian bottlenose dolphins (Gibbs et al. 2011). The arch of the premaxilla may also be linked to feeding mechanics (Rommel et al. 2009). Pterygoid shape, vertex position, nasal size, and palatine and premaxillae length may be related to sound production in different environments (Mead 2009; Mead and Fordyce 2009). The number of vertebrae (Ross 1977, 1984; Wang et al. 2000*b*; present study) can be associated with manoeuvrability (Buchholtz and Schur 2004), which in turn may reflect environmental variability (Irschick and Garland 2001).

Bottlenose dolphin species can be both sympatric and parapatric depending on the region that they inhabit (Hale et al. 2000; Wang et al. 2000*b*). *Tursiops aduncus* is generally associated with shallow water on the continental shelf, whereas *T. truncatus* is found in deep and shallow waters, both inshore and offshore (Rice 1998; Reeves et al. 2002). In several delphinid taxa, skull shape differs between inshore and offshore environments (de Araujo Monteiro-Filho et al. 2002; Jedensjö et al. 2017). In posterior view, inshore forms have crania with a rounded appearance, whereas those offshore are angular. This shape difference was observed in our study of Australian bottlenose dolphins and may be used to infer that *T. aduncus* is inshore and *T. truncatus* is offshore. In addition, some forms of pterygoid erosion are caused by nematodes (Raga et al. 1982) that are more abundant in inshore habitats (Mead and Potter 1995).

In the present study, *T. aduncus* had more pterygoid erosion than *T. truncatus*. A broad continental shelf is found off the northern coast of Australia and almost all of the specimens from this region were assigned to *T. aduncus*. Most were by-caught in the offshore gillnet fishery up to 250 km from shore (Harwood and Hembree 1987). In South Australia, the large protected gulfs may act as drivers for the small size of *T. aduncus* there. In contrast, only *T. truncatus* was identified in the shallow waters of Bass Strait, an oceanographically unique habitat separating Tasmania from mainland Australia (Wilson and Allen 1987; Bunt 1987). Sea-level changes during the last two million years have resulted in both separation and connection of Tasmania and mainland Australia (Frakes et al. 1987), raising the possibility that *T. truncatus* arrived during a sea-level rise.

Intraspecific morphological variation between widely spaced populations (Perrin 1984; Perrin et al. 1999) is problematic for taxonomy. This is particularly relevant for *T. aduncus* because populations are likely to be centred on isolated land masses. Morphological comparisons of *T. aduncus* and *T. truncatus* from the same region have found distinguishing features and meristics. However, studies vary substantially in what features are being collected, in contrast to meristic data, and therefore difficult to compare between regions. Comparison of meristic data from Australian bottlenose dolphins with those from China, Japan, and South Africa (Table 8) showed that *T. aduncus* was similar, although much smaller. A similar pattern was observed for *T. truncatus* (Ross 1977; Wang et al. 2000*b*; Kurihara and Oda 2007), with those from Australia larger than conspecifics from China, but smaller than those from Japan and South Africa.

Can. J. Zool. Downloaded from www.nrcresearchpress.com by Dr Maria Jedensjo on 06/24/20
For personal use only.

Some characters used in the present study were not effective in separating *T. aduncus* and *T. truncatus*. Future research needs to explore other characters. Genetic confirmation of species identity will assist this process, as will filling in distributional gaps and examining morphological differences within regions that may be driven by ecological factors.

Acknowledgements

Funding for this project was provided by the Australian Marine Mammal Centre (grant number 10/14 to C.M.K. and M.K.), Georges and Antoine Claraz Donation, Julius Klaus-Stiftung, and Schultz-Stiftung. We thank the curators and staff of museums for allowing access to specimens and data: R. How and C. Stevenson (Western Australian Museum, Perth), G. Dally (Museum and Art Gallery of the Northern Territory, Darwin), N. Bruce and B. Done (Museum of Tropical Queensland, Townsville), S. van Dyck and H. Janetzki (Queensland Museum, Brisbane), S. Ingleby (Australian Museum, Sydney), W. Longmore (Melbourne Museum, Victoria), K. Medlock and B. Bauer (Tasmanian Museum and Art Gallery, Hobart), C. Reid (Queen Victoria Museum and Art Gallery, Launceston), D. Stemmer (South Australian Museum, Adelaide), R. Sabin and L. Tomsett (Natural History Museum, London), and N. Lange (Museum für Naturkunde, Berlin). We thank P. Shaughnessy (South Australian Museum, Adelaide) for comments on previous drafts, as well as to C. Zollikofer and K. Isler (Department of Anthropology, University of Zurich) and I. Koch (University of Adelaide, Adelaide) for statistical support. Thanks go to reviewer E. Fordyce (University of Otago, Dunedin, New Zealand) for highly valued feedback on the manuscript.

References

Adams, D.C., Collyer, M.L., and Kaliontzopoulou, A. 2018. geomorph: software for geometric morphometric analyses. R package version 3.0.6. Available from https://CRAN.R-project.org/package=geomorph.

Amaral, A.R., Coelho, M.M., Marugán-Lobón, J., and Rohlf, F.J. 2009. Cranial shape differentiation in three closely related delphinid cetacean species: insights into evolutionary history. Zoology (Jena), **112**: 38–47. doi:10.1016/j.zool.2008.03.001. PMID:18815017.

Buchholtz, E.A., and Schur, S.A. 2004. Vertebral osteology in Delphinidae (Cetacea). Zool. J. Linn. Soc. **140**: 383–401. doi:10.1111/j.1096-3642.2003.00105.x.

Bunt, J.S. 1987. The Australian marine environment. *In* Fauna of Australia. General articles. Vol. 1. *Edited by* G.R. Dyne and D.W. Walton. Australian Government Publishing Service, Canberra. pp. 17–43.

Charlton-Robb, K., Gershwin, L.-A., Thompson, R., Austin, J., Owen, K., and McKechnie, S. 2011. A new dolphin species, the Burrunan dolphin *Tursiops australis* sp. nov., endemic to southern Australian coastal waters. PLoS ONE, **6**: e24047. doi:24010.21371/journal.pone.0024047. PMID:21935372.

Committee on Taxonomy. 2018. List of marine mammal species and subspecies. Society for Marine Mammalogy, Yarmouth Port, Mass. Available from https://marinemammalscience.org/species-information/list-marine-mammal-species-subspecies/ [accessed 25 September 2018].

de Araujo Monteiro-Filho, E.L., Monteiro, L.R., and Furtado dos Reis, S. 2002. Skull shape and size divergence in dolphins of the genus *Sotalia*: a tridimentional morphometric analysis. J. Mammal. **83**: 125–134. doi:10.1644/1545-1542(2002)083<0125:SSASDI>2.0.CO;2.

del Castillo, D.L., Segura, V., Flores, D.A., and Cappozzo, H.L. 2016. Cranial development and directional asymmetry in Commerson's dolphin, *Cephalorhynchus commersonii commersonii*: 3D geometric morphometric approach. J. Mammal. **97**: 1345–1354. doi:10.1093/jmammal/gyw101.

Environmental Systems Research Institute, Inc. 2008. ESRI data and maps 9.3. Environmental Systems Research Institute, Inc., Redlands, Calif.

Frakes, L.A., McGowran, B., and Bowler, J.M. 1987. Evolution of Australian environments. *In* Fauna of Australia. General articles. Vol. 1. *Edited by* G.R. Dyne and D.W. Walton. Australian Government Publishing Service, Canberra. pp. 1–16.

Geoscience Australia. 2004. GEODATA COAST 100K 2004. Geoscience Australia, Symonston, ACT, Australia. Available from https://www.ga.gov.au.

Gibbs, S.E., Harcourt, R.G., and Kemper, C.M. 2011. Niche differentiation of bottlenose dolphin species in South Australia revealed by stable isotopes and stomach contents. Wildl. Res. **38**: 261–270. doi:10.1071/WR10108.

Goslee, S.C., and Urban, D.L. 2007. The ecodist package for dissimilarity-based analysis of ecological data. J. Stat. Softw. **22**: 1–19. doi:10.18637/jss.v022.i07.

Hale, P.T., Barreto, A.S., and Ross, G.J.B. 2000. Comparative morphology and distribution of the *aduncus* and *truncatus* forms of bottlenose dolphin *Tursiops* in the Indian and Western Pacific Oceans. Aquat. Mamm. **26**: 101–110.

Hammer, Ø., Harper, D.A.T., and Ryan, P.D. 2001. PAST: Paleontological statistics software package for education and data analysis. Palaeontol. Electronica, **4**: 1–9.

Harwood, M.B., and Hembree, D. 1987. Incidental catch of small cetaceans in the offshore gillnet fishery in northern Australian waters: 1981–1985. Rep. Int. Whaling Comm. **37**: 363–367.

Hershkovitz, P. 1966. Catalog of living whales. U.S. Natl. Mus. Bull. No. 246.

Heyning, J.E., and Mead, J.G. 1996. Suction feeding beaked whales: morphological and observational evidence. Contrib. Sci. Nat. Hist. Mus. Los Angeles County, **464**: 1–12.

Irschick, D.J., and Garland, T. 2001. Integrating function and ecology in studies of adaptation: investigations of locomotor capacity as a model system. Annu. Rev. Ecol. Syst. **32**: 367–396. doi:10.1146/annurev.ecolsys.32.081501.114048.

Jedensjö, M., Kemper, C.M., and Krützen, M. 2017. Cranial morphology and taxonomic resolution of oceanic and coastal dolphins (Delphinidae) in Australian waters. Mar. Mamm. Sci. **33**: 187–205. doi:10.1111/mms.12356.

Kakuda, T., Tajima, Y., Arai, K., Kogi, K., Hishii, T., and Yamada, T.K. 2002. On the resident 'bottlenose dolphins' from Mikura water. Mem. Nat. Sci. Mus. Tokyo, **38**: 255–272.

Kassambara, A., and Mundt, F. 2017. factoextra: extract and visualize the results of multivariate data analyses. R package version 1.0.5. Available from https://CRAN.R-project.org/package=factoextra.

Kasuya, T. 1973. Systematic consideration of recent toothed whales based on the morphology of tympano-periotic bone. Sci. Rep. Whales Res. Inst. **25**: 1–103.

Kemper, C.M. 2004. Osteological variation and taxonomic affinities of bottlenose dolphins, *Tursiops* spp., from South Australia. Aust. J. Zool. **52**: 29–48. doi:10.1071/ZO03026.

Kingston, S.E., Adams, L.D., and Rosel, P.E. 2009. Testing mitochondrial sequences and anonymous nuclear markers for phylogeny reconstruction in a rapidly radiating group: molecular systematics of the Delphininae (Cetacea: Odontoceti: Delphinidae). BMC Evol. Biol. **9**: 245. doi:10.1186/1471-2148-9-245. PMID:19811651.

Kinze, C.C. 2018. A case for *Tursiops tursio* (Gunnerus, 1768). Lutra, **61**: 189–195.

Klingenberg, C.P. 2011. MorphoJ: an integrated software package for geometric morphometrics. Mol. Ecol. Resour. **11**: 353–357. doi:10.1111/j.1755-0998.2010.02924.x. PMID:21429143.

Kurihara, N., and Oda, S. 2007. Cranial variation in bottlenose dolphins *Tursiops* spp. from the Indian and western Pacific Oceans: additional evidence for two species. Acta Theriol. **52**: 403–418. doi:10.1007/BF03194238.

LeDuc, R.G., Perrin, W.F., and Dizon, A.E. 1999. Phylogenetic relationships among the delphinid cetaceans based on full cytochrome *b* sequences. Mar. Mamm. Sci. **15**: 619–648. doi:10.1111/j.1748-7692.1999.tb00833.x.

Long, J.H., Jr., Pabst, D.A., Shepherd, W.R., and McEllen, W.A. 1997. Locomotor design of dolphin vertebral columns: bending mechanics and morphology of *Delphinus delphis*. J. Exp. Biol. **200**: 65–81. PMID:9023994.

McGowen, M.R. 2011. Toward the resolution of an explosive radiation — a multilocus phylogeny of oceanic dolphins (Delphinidae). Mol. Phylogenet. Evol. **60**: 345–357. doi:10.1016/j.ympev.2011.05.003. PMID:21600295.

Mead, J.G. 2009. Overview beaked whales Ziphiidae. *In* Encyclopedia of marine mammals: *Edited by* F.W. Perrin, B. Wursig, and J.G.M. Thewissen. Academic Press, Amsterdam. pp. 94–97.

Mead, J.G., and Fordyce, R.E. 2009. The therian skull: a lexicon with emphasis on the odontocetes. Smithson. Contrib. Zool. No. 627, pp. 1–248. doi:10.5479/si.00810282.627.

Mead, J.G., and Potter, C.W. 1995. Recognizing two populations of the bottlenose dolphin (*Tursiops truncatus*) off the Atlantic coast of North America: morphological and ecological considerations. IBI Reports, **5**: 31–44.

Mitteroecker, P., Gunz, P., Bernhard, M., Schaefer, K., and Bookstein, F. 2004. Comparison of cranial ontogenetic trajectories among great apes and humans. J. Hum. Evol. **46**: 679–697. doi:10.1016/j.jhevol.2004.03.006. PMID:15183670.

Möller, L.M., Bilgmann, K., Charlton-Robb, K., and Beheregaray, L. 2008. Multigene evidence for a new bottlenose dolphin species in southern Australia. Mol. Phylogenet. Evol. **49**: 674–681. doi:10.1016/j.ympev.2008.08.011. PMID:18789390.

Moura, A.E., Nielsen, S.C., Vilstrup, J.T., Moreno-Mayar, J.V., Gilbert, M.T., Gray, H.W., et al. 2013. Recent diversification of a marine genus (*Tursiops* spp.) tracks habitat preference and environmental change. Syst. Biol. **62**: 865–877. doi:10.1093/sysbio/syt051. PMID:23929779.

Natoli, A., Peddemors, V.M., and Hoelzel, A.R. 2004. Population structure and speciation in the genus *Tursiops* based on microsatellite and mitochondrial DNA analyses. J. Evol. Biol. **17**: 363–375. PMID:15009270.

Nikaido, M., Piskurek, O., and Okada, N. 2007. Toothed whale monophyly reassessed by SINE insertion analysis: the absence of lineage sorting effects suggests a small population of a common ancestral species. Mol. Phylogenet. Evol. **43**: 216–224. doi:10.1016/j.ympev.2006.08.005.

Oksanen, J., Guillaume Blanchet, F., Friendly, M., Kindt, R., Legendre, P., McGlinn, D., et al. 2018. vegan: community ecology package. R package version 2.4-6. Available from https://CRAN.R-project.org/package=vegan.

Perrin, W.F. 1975. Variation of spotted and spinner porpoise (genus *Stenella*) in the eastern Pacific and Hawaii. Bull. Scripps Inst. Oceanogr. **21**: 1–206.

Perrin, W.F. 1984. Patterns of geographical variation in small cetaceans. Acta Zool. Fenn. **172**: 134–140.

Perrin, W.F., Dolar, M., Louella, L., and Robineau, D. 1999. Spinner dolphins

(*Stenella longirostris*) of the western Pacific and Southeast Asia: pelagic and shallow-water forms. Mar. Mamm. Sci. **15**: 1029–1053. doi:10.1111/j.1748-7692.1999.tb00876.x.

Perrin, W.F., Rosel, P.E., and Cipriano, F. 2013. How to contend with paraphyly in the taxonomy of the delphinine cetaceans? Mar. Mamm. Sci. **29**: 567–588. doi:10.1111/mms.12051.

Raga, J.A., Casinos, A., Filella, S., and Raduan, M.A. 1982. Notes on cetaceans of the Iberian coasts. V. *Crassicauda grampicola* Johnston and Mawson, 1941 (Nematoda) cause of injuries in the pterygoids of some specimens of *Grampus griseus*. Säugetierkd. Mitt. **30**: 315–318.

R Core Team. 2016. R: a language and environment for statistical computing. Version 3.3.1. R Foundation for Statistical Computing, Vienna, Austria. Available from https://www.r-project.org/.

Reeves, R.R., Stewart, B.S., Clapham, P.J., and Powell, J.A. 2002. The guide to marine mammals of the world. Alfred A. Knopf. Inc., New York.

Rice, D.W. 1998. Marine mammals of the world: systematics and distribution. The Society for Marine Mammalogy, Allen Press, Lawrence, Kans.

Rommel, S.A., Pabst, D.A., and McLellan, W.A. 2009. Skull anatomy. *In* Encyclopedia of marine mammals. 2nd ed. *Edited by* F.W. Perrin, B. Würsig, and J.G.M. Thewissen. Academic Press, Amsterdam. pp. 1033–1047. doi:10.1016/B978-0-12-373553-9.X0001-6.

Ross, G.J.B. 1977. The taxonomy of bottlenose dolphins *Tursiops* species in South African waters, with notes on their biology. Ann. Cape Prov. Mus. Nat. Hist. **11**: 135–194.

Ross, G.J.B. 1984. The smaller cetaceans of the south-east coast of southern Africa. Ann. Cape Prov. Mus. (Nat. Hist.) **15**: 173–410.

Ross, G.J.B., and Cockcroft, V.G. 1990. Comments on the Australian bottlenose dolphin and the taxonomic status of *Tursiops aduncus* (Ehrenberg, 1832). *In* The bottlenose dolphin. *Edited by* S. Leatherwood and R.R. Reeves. Academic Press, San Diego, Calif. pp. 101–128.

Schlager, S. 2017. Morpho and Rvcg — Shape analysis in R. *In* Statistical shape and deformation analysis. *Edited by* G. Zheng, S. Li, and G. Szekely. Academic Press, London. pp. 217–256.

van Etten, J. 2015. gdistance: distances and routes on geographical grids. Version 1.1-9. Available from https://CRAN.R-project.org/package=gdistance.

Venables, W.N., and Ripley, B.D. 2002. Modern applied statistics with S. Springer, New York.

Wang, J.Y., Chou, L.-S., and White, B.N. 2000*a*. Differences in the external morphology of two sympatric species of bottlenose dolphins (genus *Tursiops*) in the waters of China. J. Mammal. **81**: 1157–1165. doi:10.1644/1545-1542(2000)081<1157:DITEMO>2.0.CO;2.

Wang, J.Y., Chou, L.-S., and White, B.N. 2000*b*. Osteological differences between two sympatric forms of bottlenose dolphin (genus *Tursiops*) in Chinese waters. J. Zool. **252**: 147–162. doi:10.1111/j.1469-7998.2000.tb00611.x.

Wells, R.S., and Scott, M.D. 1999. Bottlenose dolphin *Tursiops truncatus* (Montagu, 1821). *In* Handbook of marine mammals. Vol. 6. *Edited by* S.H. Ridgway. Academic Press, San Diego, Calif. pp 137–182.

Wilson, B.R., and Allen, G.R. 1987. Major components and distribution of marine fauna. *In* Fauna of Australia. General articles. Vol. 1. *Edited by* G.R. Dyne and D.W. Walton. Australian Government Publishing Service, Canberra. pp. 156–184.

Appendix A

Table A1. Abbreviations and their definitions used throughout text, figures, and tables are listed in alphabetical order.

Abbreviation	Definition
2D	Two-dimensional data
3DGM	Three-dimensional geometric morphometrics data
DFA	Discriminant function analysis
GPA	Generalised Procrustes analysis
HCA	Hierarchical cluster analyses
MANOVA	Multivariate analysis of variance
MS	Mean squares
NSW	New South Wales
NT	Northern Territory
PCA	Principal component analysis
PCs	Principal components
PERMANOVA	Permutational multivariate analysis of variance
QLD	Queensland
SA	South Australia
SABD	Southern Australian bottlenose dolphin
SS	Sum of squares
TAS	Tasmania
TPS	Thin-plate-spline
UPGMA	Unweighted pair-group method with arithmetic averaging
VIC	Victoria
WA	Western Australia

Can. J. Zool. Downloaded from www.nrcresearchpress.com by Dr Maria Jedensjo on 06/24/20
For personal use only.

Table A2. Two-dimensional skull measurements for bottlenose dolphin (*Tursiops* spp.) specimens examined in this study.

Variable	Direction of measurement	References
CBL: condylobasal length	1	WP, GR, JYW, CK
RL: rostrum length	1	WP, GR, JYW, CK
TREN: tip of rostrum to external nares	1	WP, GR, JYW, CK
RWB: rostrum width at base	3	WP, JYW, CK
RW60: rostrum width at 60 mm from base	3	WP, GR, CK
RW75%: rostrum width at 3/4 of rostrum length from base	3	WP, GR, JYW, CK
RWM: rostrum width at mid-length	3	WP, GR, CK
RW25%: rostrum width at 1/4 of rostrum length from base	3	JYW
PRW: premaxillae width at mid-rostral length	3	WP, GR, JYW, CK
WCB: width of cancellous bone on maxilla at mid-rostrum	2	CK
PAB: apex of premaxillary convexity to base	1	JYW
GPRW: greatest preorbital width of skull	3	WP, GR, JYW, CK
LSOW: least supraorbital width	3	WP, JYW
GWPRX: greatest width right premaxillae	3	#MJ
GWLPX: greatest width left premaxillae	2	#MJ
GWPX: greatest width of premaxillae	2	WP, GR, JYW, CK
WRN: greatest width of right nasal	2	#MJ
HRN: greatest height of right nasal	2	#MJ
WLN: greatest width of left nasal	2	#MJ
HLN: greatest height of left nasal	2	#MJ
GWEN: greatest width of external nares	3	WP, GR, JYW, CK
GWAO: greatest width of anterior overhang of nuchal crest	2	CK
ZW: zygomatic width of skull	3	WP, GR, JYW, CK
GPOW: greatest postorbital width of skull	3	WP, GR, JYW, CK
GPARW: greatest width across parietals	3	WP, GR, JYW, CK
LWPTF: least width between posterior borders of temporal fossa	3	CK
EHB: external height of braincase	2	GR
EHBHP: external height of braincase to highest point	2	#MJ
ILB: internal length of braincase, from occipital condyles to anterior wall of cranium	2	GR, CK
GLPTF: greatest length of left temporal fossa	2	WP, GR, CK
GWPTF: greatest width of left temporal fossa	2	WP, GR, CK
MAJDTF: major diameter of (anterior) temporal fossa	2	WP, CK
MINDTF: minor diameter of (anterior) temporal fossa	2	WP, CK
LO: length of orbit	2	WP, GR, JYW, CK
LAL: length of antorbital process of lacrimal	2	WP, JYW, CK
GWIN: greatest width of internal nares	3	WP, JYW, CK
GLPT: greatest length of pterygoids	2	WP, JYW, CK
TRPS tip of rostrum to medial palatine suture	1	#MJ
UTLTR: length of upper tooth row to tip of rostrum	1	WP, GR, JYW, CK
ATW: alveolar tooth width at mid-rostrum	2	JYW
WAS: width of alisphenoid at suture with the basisphenoid	3	JYW
GWPV: greatest width of posterior flange of the vomer	3	JYW, CK
ML: mandible length	1	WP, GR, CK
LTRL: length of lower tooth row to tip of rostrum	1	WP, GR, JYW, CK
MH: mandible height	2	WP, GR, JYW, CK
MSL: mandibular symphysis length	1	CK
MFL: mandibular fossa length	2	WP, JYW, CK
APDC: antero-posterior diameter of cochlear portion of periotic	1	TK
LT: length of tympanic bulla	1	TK, GR, CK
ATEIP: anterior tip to end of inner posterior prominence	1	TK
WT: width of tympanic bulla	3	TK
WIOP: width across inner and outer posterior prominence of bulla	3	TK
TD: tooth diameter	NA	CK

Note: Direction of variable measurement is either parallel to plane of view (1), parallel to feature (2), perpendicular to plane (3), or not applicable (NA). Variables are described in WP (Perrin 1975), GR (Ross 1977), JYW (Wang et al. 2000*b*), CK (Kemper 2004), TK (Kasuya 1973), and #MJ (new measurement).

Can. J. Zool. Downloaded from www.nrcresearchpress.com by Dr Maria Jedensjo on 06/24/20
For personal use only.

Table A3. Categorical skull and tooth data and vertebral counts for bottlenose dolphin (*Tursiops* spp.) specimens used in this study.

Data	Codes	Reference
Bone resorption to frontal and pterygoids (possibly parasite related)	1 (none), 2 (slight), 3 (moderate erosion), 4 (extensive erosion)	CK
Extent of the nuchal crest	0 mm (none), 1–5 mm (slight), 6–10 mm (moderate), >10 mm (large)	CK
Temporal fossa shape (length/width)	1 (oval), 2 (round)	CK
Highest point of skull	1 (nuchal crest), 2 (interparietal of vertex), 3 (frontal), 4 (nasal)	CK
Pterygoid hamular ridge shape	1 (no ridge), 2 (slight ridge or ridge just at anterior end), 3 (distinct ridge all along the pterygoid)	CK
Pterygoid convexity (in anterior view)	1 (flat), 2 (slight to moderate), 3 (very arched)	CK
Arch of premaxilla along the rostrum	1 (flat), 2 (slight to moderate), 3 (very arched)	CK
Position of lower tip of pterygoid vs. top maxilla suture	1 (suture lower than pterygoid tip), 2 (suture and pterygoid tip same height), 3 (suture higher than pterygoid tip)	KCR
Pterygoid to maxilla suture	1 (maxilla suture closer to tip of rostrum compare with the pterygoid tip), 2 (same distance), 3 (suture farther away from tip of rostrum compare with the pterygoid tip)	KCR
Palatine shape	1 (even triangle shape), 2 (skewed triangle shape), 3 (prolonged triangle shape)	KCR
Comparison of pterygoid and palatine length	1 (pterygoid longer), 2 (palatine longer), 3 (pterygoid and palatine same length)	KCR
Tooth counts	TUL (number of teeth upper left), TUR (number of teeth upper right), TLL (number of teeth lower left), TLR (number of teeth lower right)	CK
Vertebral counts	CV (cervical), TV (thoracic), XV (lumbar), YV (anterior caudal), Z (posterior caudal), TOTV (total vertebrae), VPVF (number of first vertebra with perforating vertical foramen)	CK

Note: Variables are described in CK (Kemper 2004) and KCR (Charlton-Robb et al. 2011).

Table A4. Three-dimensional landmarks for bottlenose dolphin (*Tursiops* spp.) specimens examined in this study.

Landmark	Definition
1–2	Tip of rostrum left and right side
3–4	Rostrum width at 3/4 from base on left and right side
5–6	Rostrum width at mid-length from base on left and right side
7–8	Rostrum width at 1/4 from base on left and right side
9–10	Rostrum width at narrowing on left and right side
11 and 14	Preorbital point on left and right side
12–13	Rostrum base on left and right side
15–16	Greatest preorbital width of cranium on left and right side
17–18	External nares lower on left and right side
19–20	Greatest width of external nares on left and right side
21–22	Highest point of nasal on left and right side
23 and 27	Corner of crest left and right side
24 and 26	Halfway point between landmarks 23–35 and 25–27, respectively, measured on nuchal crest
25	Midpoint of nuchal crest
28	Mid-length between opening upper and midpoint of crest
29 and 33	Greatest postorbital width of cranium on left and right side
30 and 34	Zygomatic width of cranium on left and right side
31 and 35	Greatest width between temporal fossa on left and right side
32 and 36	Least width between posterior border of temporal fossa on left and right side
37 and 41	Greatest width of left occipital condyles on left and right side
38 and 40	Greatest width opening left and right side
39 and 42	Greatest height upper left and right side
43	Greatest height of cranium
44 and 53	Apex of premaxilla on left and right side
45 and 52	Mid-length orbit on left and right side
46 and 50	Greatest height of temporal fossa upper on left and right side
47 and 51	Greatest height of temporal fossa lower on left and right side
48–49	Greatest length of cranium at the occipital condyles on left and right side
54	Medial palatine suture
55–56	Mid-length on pterygoid crests on right and left side
57 and 59	Tip of pterygoids on left and right side
58	Pterygoid angle
60–61	Greatest width of internal nares on left and right side
62 and 66	Width of alisphenoid at suture with the basisphenoid on left and right side
63 and 65	Mid-length between alisphenoid at suture and basisphenoid on left and right side
64	Midpoint of basisphenoid
67 and 71	Highest point of basioccipital on left and right side
68 and 70	Mid-length between midpoint and highest point of basioccipital on left and right side
69	Midpoint basioccipital
72–73	Highest point paraoccipital

Can. J. Zool. Downloaded from www.nrcresearchpress.com by Dr Maria Jedensjo on 06/24/20
For personal use only.